Impact of sources and form of Mg on oyster shell Mg/Ca

Marie Pesnin[1,2*], Laurent Emmanuel[1], Amélie Guittet[1], Boris Eyheraguidel[3], Gaëtan Schires[4], Julien Normand[5], Vincent Mouchi[6,7,8]

[1]: Sorbonne Université, CNRS-INSU, Institut des Sciences de la Terre Paris, ISTeP, F-75005, Paris, France

[2]: Geowissenschaftliches Zentrum, Georg–August–Universität Göttingen, 37077, Göttingen, Germany.

[3]: Institut de Chimie de Clermont-Ferrand, Campus universitaire des Cézeaux, 63178, Aubière, France

[4]: Station Biologique de Roscoff, CNRS-Sorbonne Université, Roscoff 29682, France.

[5]: Ifremer, Laboratoire Environnement Ressources de Normandie, Avenue du Général de Gaulle, 14520, Port-en-Bessin, France

[6]: Sorbonne Université, CNRS, Adaptation et Diversité en Milieu Marin, AD2M, Station Biologique de Roscoff, 29680, Roscoff, France

[7]: CNRS, CReAAH, Université de Rennes, Rennes Cedex, France

[8]: Sorbonne Université, CNRS, Laboratoire d'Ecogéochimie des Environnements Benthiques, LECOB, Observatoire Océanologique, F-66650, Banyuls-sur-mer, France

[*]Corresponding author: marie.pesnin@uni-goettingen.de

Impact of sources and form of Mg on oyster shell Mg/Ca

Marie Pesnin[1,2*], Laurent Emmanuel[1], Amélie Guittet[1], Boris Eyheraguidel[3], Gaëtan Schires[4], Julien Normand[5], Vincent Mouchi[6,7,8]

[1]: Sorbonne Université, CNRS-INSU, Institut des Sciences de la Terre Paris, ISTeP, F-75005, Paris, France

[2]: Geowissenschaftliches Zentrum, Georg–August–Universität Göttingen, 37077, Göttingen, Germany.

[3]: Institut de Chimie de Clermont-Ferrand, Campus universitaire des Cézeaux, 63178, Aubière, France

[4]: Station Biologique de Roscoff, CNRS-Sorbonne Université, Roscoff 29682, France.

[5]: Ifremer, Laboratoire Environnement Ressources de Normandie, Avenue du Général de Gaulle, 14520, Port-en-Bessin, France

[6]: Sorbonne Université, CNRS, Adaptation et Diversité en Milieu Marin, AD2M, Station Biologique de Roscoff, 29680, Roscoff, France

[7]: CNRS, CReAAH, Université de Rennes, Rennes Cedex, France

[8]: Sorbonne Université, CNRS, Laboratoire d'Ecogéochimie des Environnements Benthiques, LECOB, Observatoire Océanologique, F-66650, Banyuls-sur-mer, France

[*]Corresponding author: marie.pesnin@uni-goettingen.de

Abstract

Mg/Ca in bivalve shells has been investigated as a promising temperature proxy, but several studies reported compositional shifts that hamper its accuracy. In particular, several models linking shell Mg/Ca and temperature have been published and an empirical difference in the seasonal amplitudes of shell Mg/Ca has been observed between two types of environmental settings: river output, open marine. Here, we investigate several environmental parameters that could be responsible for this difference, using rearing experiments of oysters in natural and artificial seawater. We first tested the influence of Mg form in seawater on shell Mg/Ca and showed that Mg is incorporated in shell regardless of it form (complexed and free). Second, we investigated the sensitivity of shell Mg/Ca to seawater Mg/Ca by artificially increasing the Mg content in seawater. We observe an increase in shell Mg/Ca with seawater Mg/Ca, as previously suggested. Finally, we show that a change in diet induces a significant difference in shell Mg/Ca. Overall, our results suggest that, besides temperature, seawater and food Mg/Ca control shell Mg/Ca. These parameters could be responsible for the discrepancy of Mg/Ca-temperature models, and should be considered for future aquarium and in situ calibration studies, as well as paleoenvironmental reconstructions.

1. Introduction

Present climates are defined by both the means and variabilities of environmental parameters over a period of 30 years (WMO, 2025). Reconstructing past climates therefore requires paleoenvironmental archives with compatible temporal resolution. Unlike sedimentary records, climatic cycles within the carbonate shell of marine molluscs occur with a temporal resolution ranging from multi-year cycles to tidal cycles (Chauvaud et al., 2005; Lartaud et al., 2010a; Huyghe et al., 2019; Mouchi et al., 2025a). The study of these high-frequency paleoenvironmental records is necessary to refine the temporal resolution of past climate models that will help us understand future environmental changes. Bivalves are capable of recording, within their shells, variations in the physicochemical parameters controlling their living environment such as temperature (e.g., Epstein et al, 1953; Purton and Brasier, 1997; Kirby et al., 1998; Vander Putten et al., 2000; Mouchi et al., 2013; Huyghe et al., 2015, Briard et al., 2020; Uvanovic et al., 2021).

Paleoclimatologists generally rely on the oxygen isotope ratios ($\delta^{18}O$) of calcium carbonate shells to access temperature from ancient times. Assuming that the precipitation of carbonate shell in bivalve occurs in equilibrium with seawater, the fluctuations of isotopic ratios recorded throughout the growth therefore reflect those of seawater (e.g., Urey et al., 1951; Wefer and Berger, 1991; Ullmann et al., 2010; Tynan et al., 2014). It has been shown that shell $\delta^{18}O$ depends on water temperature and seawater $\delta^{18}O$, which covaries with salinity (Lartaud et al., 2010b, Pierre., 1999). However, estimating past salinity values in coastal areas is often imprecise and complex (Rohling, 2000). Other geochemical markers, dependent solely on temperature, are therefore being investigated to faithfully reconstruct seawater temperature variations in coastal environments. Among these markers, Mg/Ca ratio of bivalves has been extensively studied to estimate past seawater temperature variations (e.g., Klein et al., 1996; Vander Putten et al., 2000; Surge & Lohmann, 2008; Bougeois et al., 2016; Tynan et al., 2017; Mouchi et al., 2018, Hausmann et al., 2024). However, this paleo-climatic proxy is also known to be controlled by other factors (e.g., pH and specimen age; Lazareth et al., 2007; Surge & Lohmann, 2008; Mouchi et al., 2013; Schöne & Gillikin, 2013; Hausmann et al., 2017), making its interpretation in terms of climatic conditions challenging. Large variability has been reported in both shell Mg/Ca absolute values and the correlation between temperature and shell Mg/Ca (Freitas et al., 2008; Wanamaker et al., 2008; Tynan et al., 2017; Mouchi et al., 2018; Schleinkofer et al., 2021; Mouchi et al., 2025b; **Figure 1**). Very limited impact of salinity has been reported (Mouchi et al., 2013), although previous studies have highlighted that the Mg/Ca ratio of bivalve shells differ between purely marine environments (open marine) and estuarine and bay environments (Mouchi et al., 2018; **Figure 1**). As Mg is one of the most common cations in seawater, its availability should be increased in open marine settings compared to coastal areas with freshwater input. However, observations indicate that estuarine bivalves present a higher Mg/Ca than those of marine settings (Mouchi et al., 2018). Several reasons can be advanced to explain this discrepancy. Changes in seawater Mg/Ca with the environment has been suggested by Tynan et al. (2017) as one of these reasons. Another possibility could be the bio-availability of Mg. In theory, Mg in seawater can exist in two forms: the free ionic form (Mg^{2+}) and the complexed form. Indeed, Mg^{2+} ions present in seawater can be complexed either by inorganic (OH^{+}, SO_4, CO_3) or organic compounds (carboxylic

86 acids, carbohydrates, amino acids, phenolic compounds) through covalent bounds
87 (Hirose. 2006). Although the nature and origin of these organic ligands remain largely
88 unknown, by analogy with Fe, these organic ligands can be classified into two main
89 groups: ligands produced by photoautotrophic microorganisms and ligands derived from
90 the degradation of organic matter (Chipmann, 1966; Marchand et al., 1974; Hunter and
91 Boyd, 2007). The proportion of the two forms of Mg in seawater has never been directly
92 measured. Indeed, conventional methods for measuring Mg in seawater, which generally
93 involve plasma ionization (ICP-OES, ICP-AES, ICP-MS; Surge & Lohmann, 2008; Tynan et
94 al., 2017), quantify the total Mg in a solution, regardless of its form. However, studies have
95 shown a positive gradient in dissolved organic matter concentration in seawater from
96 estuarine to open marine environments (Le Corre et al., 1972; Wafar and Le Corre, 1982,
97 Zhang et al., 2019). It is accepted that the greater the density of organic ligands in a
98 medium, the more favourable that medium becomes for the formation and maintenance
99 of organometallic complexes (Zhang et al., 2019). Thus, we can assume that seawater in
100 open marine environments is richer in complexed Mg than that in estuarine
101 environments. Recent work of Mavromatis et al. (2017) have demonstrated that due to
102 adsorption onto the calcite surfaces and the subsequent reduction of the active sites of
103 growth, the presence of Mg-organic-complex promotes the incorporation of Mg into
104 abiogenic calcite. Nevertheless, the effect of such organic ligands on Mg incorporation
105 into biogenic calcite has not yet been investigated. It is possible that their impact differs
106 significantly in biological systems. In particular, Mg complexed with organic ligands is
107 likely not directly accessible to organisms for incorporation into their shells, as it must
108 first cross the cellular barrier and undergo enzymatic decomposition to return to its free
109 form (Shaked & Lis, 2012). These enzymatic processes are energetically costly, and
110 bivalves may therefore preferentially incorporate free Mg, which requires less energy.
111 Another possible reason to explain the high shell Mg/Ca in estuarine settings compared
112 to open marine would be the food source, if Mg content is higher depending on the
113 plankton species. To assess the bioavailability of Mg in seawater for bivalves, we propose
114 to examine the potential sources of Mg incorporated into the shells of the oyster species
115 *Magallana gigas* through a 7-month aquarium experiment at two French sites: in Paris
116 (Sorbonne Université - ISTeP) with artificial seawater, and at the Biological Station of
117 Roscoff (Sorbonne Université - AD2M) with natural seawater. Due to their rapid growth

and the excellent preservation of their shells against alteration and/or diagenesis effects, oysters seem particularly well-suited for paleoenvironmental reconstructions (Mouchi et al., 2025a) and have therefore been chosen for this experiment. The temperature and salinity of the aquarium water will be maintained constant throughout the experiment. Three sources of Mg incorporation into the shells will be tested: (1) enriched free Mg^{2+} from seawater, (2) enriched complexed Mg from seawater, and (3) Mg from diet.

Seawater analyses from the culture media will be conducted using inductively coupled plasma optical emission spectrometry (ICP-OES) and ion exchange chromatography (IEC) to assess the proportions of complexed and free Mg in seawater. The chemical composition of the shells will be analysed in situ using laser ablation-inductively coupled plasma mass spectrometry (LA-ICP-MS). The Mg concentrations in these shells will be compared to identify the preferred source of the Mg incorporated into the shells. Overall, the results of this experiment will contribute to a better use of the Mg/Ca proxy by providing new information on parameters other than temperature influencing the Mg/Ca ratio in bivalves.

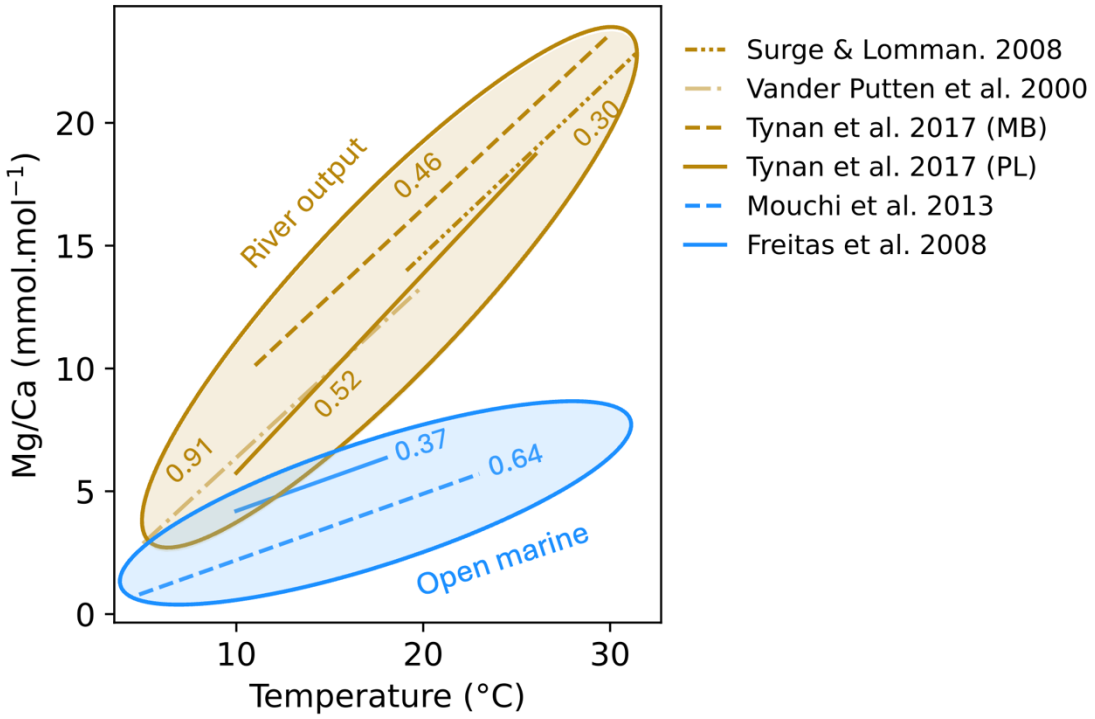

Figure 1: Existing calibrations of calcitic bivalve shell Mg/Ca in relation to seawater temperature. For each model, the correlation coefficient r^2 is indicated. Two clusters of

models are visible: river output (dark gold) or open marine (blue) environments. For Tynan et al. (2017) models, MB correspond to the Moreton Bay and PL is Pambula Lake.

2. Materials

2.1. *Magallana gigas* specimens

The rearing experiment was perfomed on specimens of *Magallana gigas*. These oysters, originating from spatfall, had initially been reared in the Baie des Veys (49°22'35" N, 1°08'20" W) in the southern English Channel. A total of 300 one-year-old individuals were collected alive and transferred to aerated seawater tanks to ensure their survival during transportation to the rearing sites. The individuals were then randomly assigned to one of two culture sites of Sorbonne University: Biological Station of Roscoff (SBR, Roscoff Aquarium Services) and the Institute of Earth Sciences of Paris (ISTeP). The oysters were maintained in natural seawater (NSW) at Roscoff, while they were reared in artificial seawater (ASW) at Paris. Each oyster was labelled with a unique identification number using micro-labels affixed to the shell (Hallprint Glue-on Shellfish Tags type FPN 8x4 mm), with specimens in natural seawater (Roscoff) numbered G.000 to G.150 and those in artificial seawater (Paris) numbered G.300 to G.450 (**SI 1**).

2.2. Rearing strategy

2.2.1. General settings

Three tanks with a capacity of 30 liters at Paris (P1, P2, P3) and 100 liters at Roscoff (R1, R2/R4, R3) were set up to accommodate *M. gigas* individuals collected on the field (**Figure 2**). At Roscoff, the tanks were filled with natural seawater pumped offshore (48°43'39" N, 3°59'15" W), while at Paris the tanks were supplied with artificial seawater. The ASW was prepared by dissolving synthetic sea salt (Instant Ocean) in deionized water produced by reverse osmosis. The amount of Instant Ocean salt added to the solution was chosen to archive a salinity of 35 matching that of natural seawater at Roscoff. Furthermore, to limit salinity fluctuations due to evaporation, perforated lids were placed on the top of each tank at the Paris rearing site (**Figure 2a**).

Twice a week, 10% to 17% of the ASW and NSW was renewed to maintain a stable Mg concentration. In addition, at Paris a full water renewal and cleaning of the tank was performed once a month to remove organic waste and prevent from nitrite accumulation. To ensure proper water oxygenation of the ASW, all tanks were equipped with mixing units (**Figure 2a**). The mixing was programmed in water flow intensity following a day/night cycle to mimic natural variations. In contrast, at the Roscoff site, water circulation was achieved through a two-level mechanical overflow system (**Figure 2b**). This system allowed water to flow from the rearing aquarium to a recovery tank equipped with pre-colonized bacterial filter, from which seawater was pumped back to the rearing aquarium.

In order to minimize fluctuations of seawater temperature thought the experimental period, the rearing tank were installed in an air-conditioned room. The air-conditioning system was set to maintain the tank's seawater temperature around 20°C. This value of temperature also corresponds to that at which the discrepancy between Mg/Ca-temperature calibrations reported in the literature becomes more pronounced (**Figure 1**).

At the beginning of the experiment, each tank received 30 individuals of *M. gigas*, with additional specimens kept in holding tanks as replacements in case of mortality. Except for specimens reared in tank R4, all *M. gigas* individuals were fed daily with 1 mL of concentrated Instant Algae solution (Instant Algae© Shellfish Diet 1800). This planktonic mixture is composed of *Tetraselmis* sp., *Thalassiosira weissflogii*, and *Thalassiosira pseudonana* (all <20 µm in size).

Immediately, at the beginning of the experiment, in vivo Mn labeling of all specimens was performed to locate the experimental period in the shell, following the protocol described in Lartaud et al. (2010). Specimens were introduced into a temporary tank filled with seawater enriched in $MnCl_2$ (total concentration: 90 $mg.L^{-1}$) for 4.5h. Additional Mn labels were performed throughout the experimental period (**Table S1 and S2**) to follow shell growth.

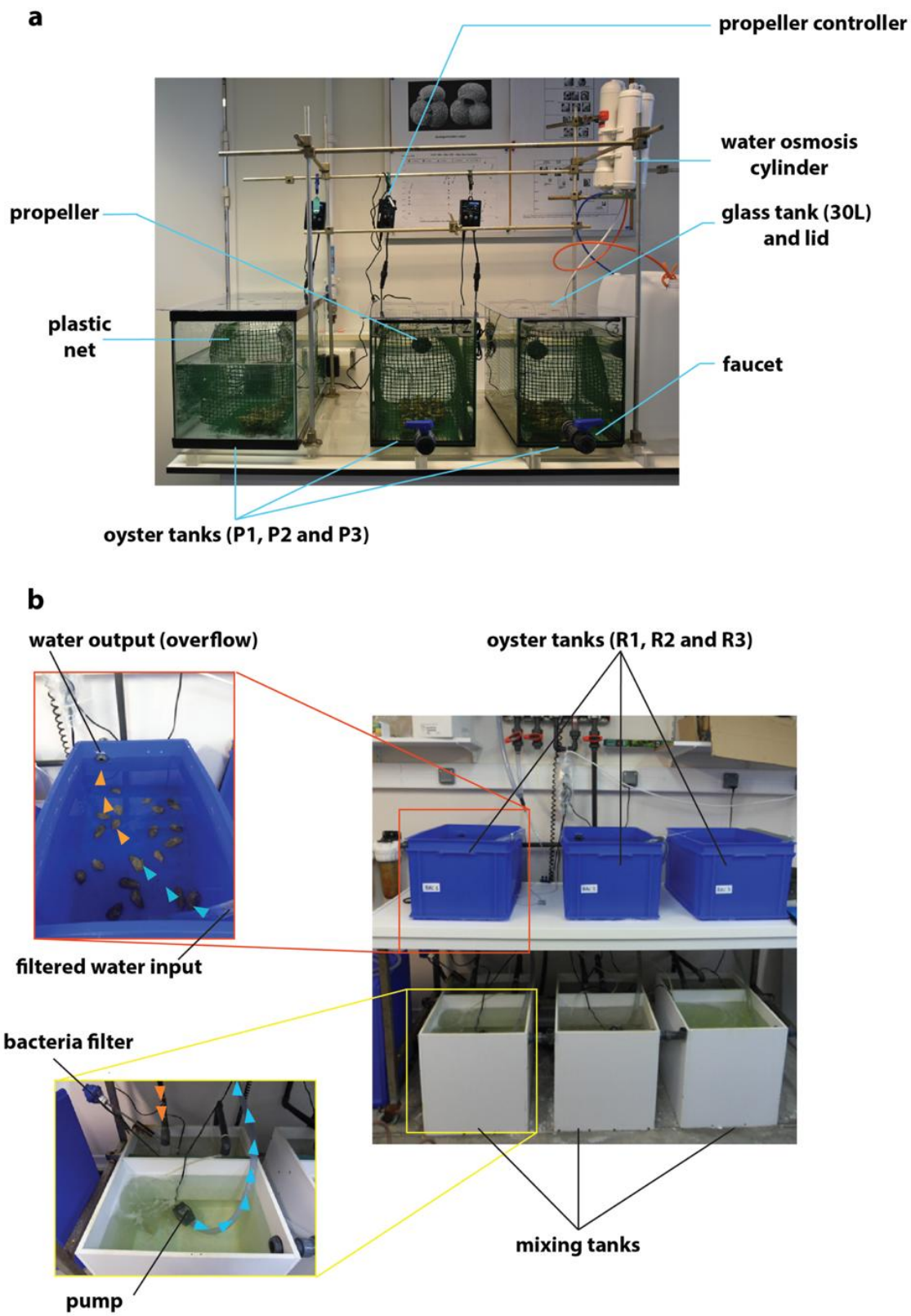

Figure 2: Experimental settings at Paris (a) and Roscoff (b).

2.2.2. Experimental conditions

At each site, in addition to a control tank, two tanks were used to test the impact of different Mg sources on the shell Mg/Ca record (**Figure 3a**).

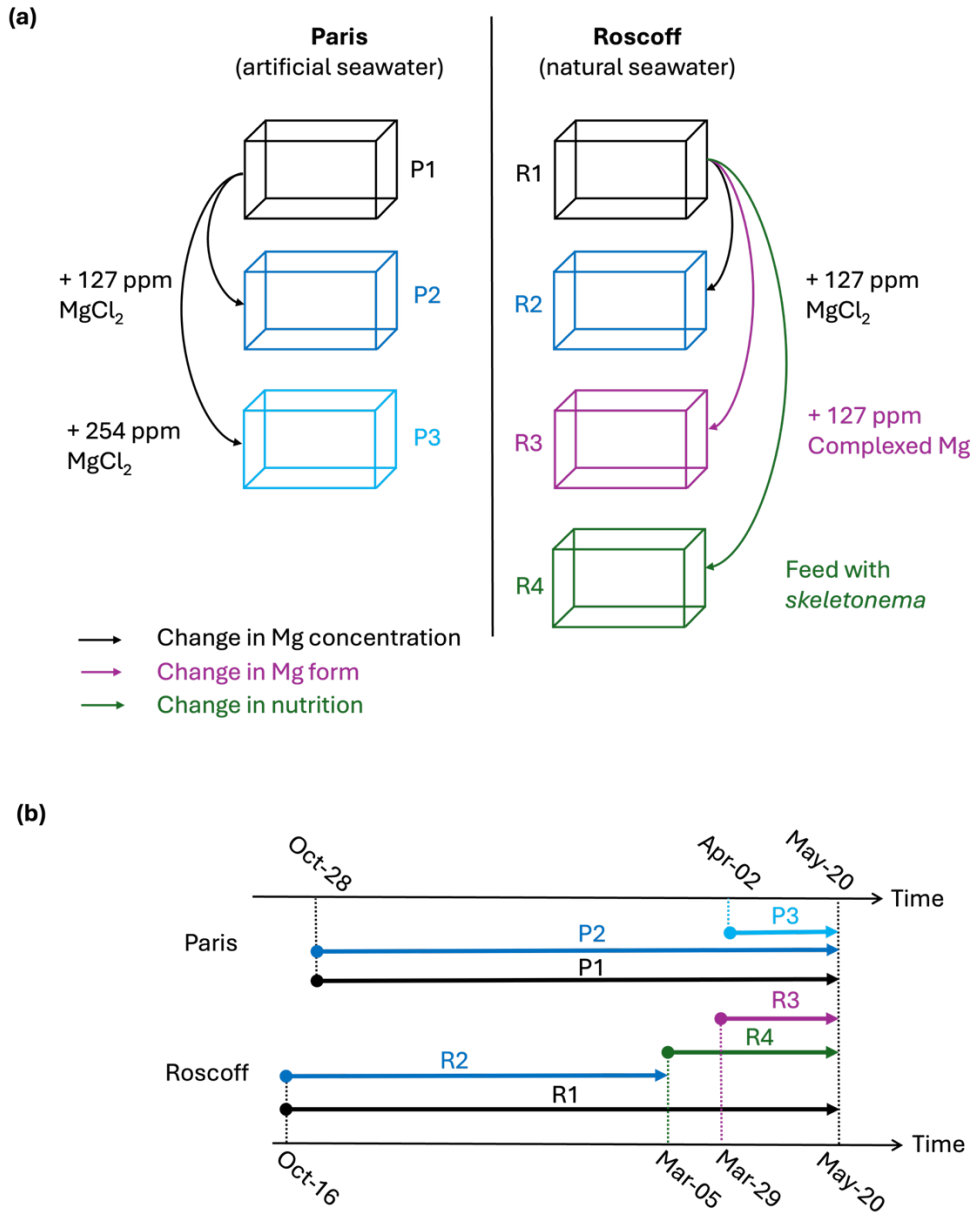

Figure 3: Summary of experimental oyster rearing conditions (a) Schematic representation of experimental rearing conditions for oysters at the Paris and Roscoff sites. **(b)** Gantt chart illustrating the experimental conditions applied to *M. gigas* rearing tanks over the course of the experiment.

2.2.2.1. Seawater enriched with free Mg

In the first experimental condition, we tested whether the Mg concentration of the seawater affects the Mg/Ca ratio of *M. gigas* shells. For this purpose, the Mg concentration of the seawater in tank P2 (Paris) and R2 (Roscoff) was artificially increased by 127 ppm relative to the control condition P1 and R1 (**Figure 3a**). To maintain this enrichment, a solution of $MgCl_2$ (99% anhydrous magnesium chloride) was prepared in 100 mL of artificial seawater (or natural seawater at Roscoff) and added to the aquariums during each water renewal. An additional condition was introduced later in the year (April 2, 2021), at the Paris site, in tank P3, where the Mg concentration was further increased to 254 ppm, while the conditions in P2 remained unchanged (**Figure 3**).

2.2.2.2. Seawater enriched with complexed Mg

In the second experimental condition we examined the effect of Mg form on the efficiency of its incorporation in *M. gigas* shells. To this end, tank R3 at Roscoff was enriched with complexed Mg by 127 ppm. This was archived by using a magnesium-EDTA complex solution (TCI, ref. E0094), added to the tank at each water renewal (**Figure 3a**).

2.2.2.3. Different food supply

In the last experimental condition, we investigate whether diet can influence the shell Mg/Ca by modifying the oyster's feeding regimen. To test this, a new condition, R4, was established in tank R2 (**Figure 3**). In practice, on March 5, 2021, Mg enrichment in R2 was stopped. The R2 tank was emptied, thoroughly rinsed, and refilled with filtered natural seawater. From this point onward, oysters in this tank were fed with a fresh mono-specific culture of *Skeletonema* sp., a diatom species naturally consumed by oysters (Pouil et al., 2020), grown at the Biological Station of Roscoff. The magnesium content of this *Skeletonema. sp* solution was measured using ICP-OES and compared to that of the *Instant Algae* used in other conditions.

2.2.2.4. Control conditions

Control conditions were established in tanks P1 and R1, which did not receive any artificial Mg enrichment. *Magallana gigas* individuals raised in these control tanks were maintained under the same environmental conditions (temperature and salinity) and

feeding regimen (i.e, *Instant Algea*) as those in the experimental tanks (apart from tank R4), allowing for direct comparison between conditions.

2.2.3. Monitoring of rearing conditions

The rearing experiment started on October 28, 2020, at the Paris site and November 16, 2020, at the Roscoff site (**Figure 3b**). From these start dates and over the 7-month experimental period, a daily monitoring of seawater temperature, salinity, and oyster mortality was conducted in each tank (**SI 2 and 3, Supplementary Table S1 & Table S2**). Regular sampling of seawater was also performed to check the stability of Mg enrichment and to evaluate the influence of water renewal on seawater Mg concentrations. In addition, we also tracked the evolution of shell growth rate throughout the experiment using in vivo Mn^{2+} labeling and cathodoluminescence imaging.

3. Methods

3.1. Shell sample preparation and locating Mn markings

Magallana gigas specimens were taken out from rearing tanks for geochemical analysis at different stages of the culture experiment. Immediately after collection, the oysters were opened, their soft tissues removed, and the shells rinsed with deionized water. To ensure shell preservation and eliminate residual organic matter, shells were treated overnight with a 15% hydrogen peroxide (H_2O_2) solution and then rinsed thoroughly with demineralized water.

For geochemical analysis, we focused on the hinge area rather than the entire shell, as it retains the organism's growth history within a single, well-defined portion (Langlet et al., 2006; Lartaud et al., 2010a). The umbo of each left valve was excised and embedded in Huntsman Araldite 2020 epoxy resin. A longitudinal thick section was then cut along the maximum growth axis, extending from the hinge region to the ventral shell margin, revealing the growth increments. The resulting thin sections were polished to a final thickness of ~300 µm using alumina powder. All geochemical analyses were conducted on the foliated calcite region of the hinge sections.

To locate Mn markings withing *M. gigas* shells, we performed cathodoluminescence (CL) microscopy following the method describe in Lartaud et al. (2010). CL observations were conducted using a cold cathode (Cathodyne-OPEA) at ISTeP, with settings of 15–20 keV and 200–400 µA.mm^{-2} under a pressure of 0.05 Torr. Luminescence images were captured with a Nikon D5000 camera (1400 ASA) using a 20-second exposure time. In calcite, Mn^{2+} incorporation during mineral growth produces a characteristic CL emission at ~620 nm, appearing as bright red luminescence (**Figure 4a**). The Mn markings identified via CL microscopy were cross-referenced with Mn content variations determined by LA-ICP-MS (**Figure 4b**). Given that umbo growth reflects overall shell growth (Lartaud et al., 2010a), we used Mn marking dates in combination with CL observations to determine shell growth rates under rearing conditions (**SI 3**).

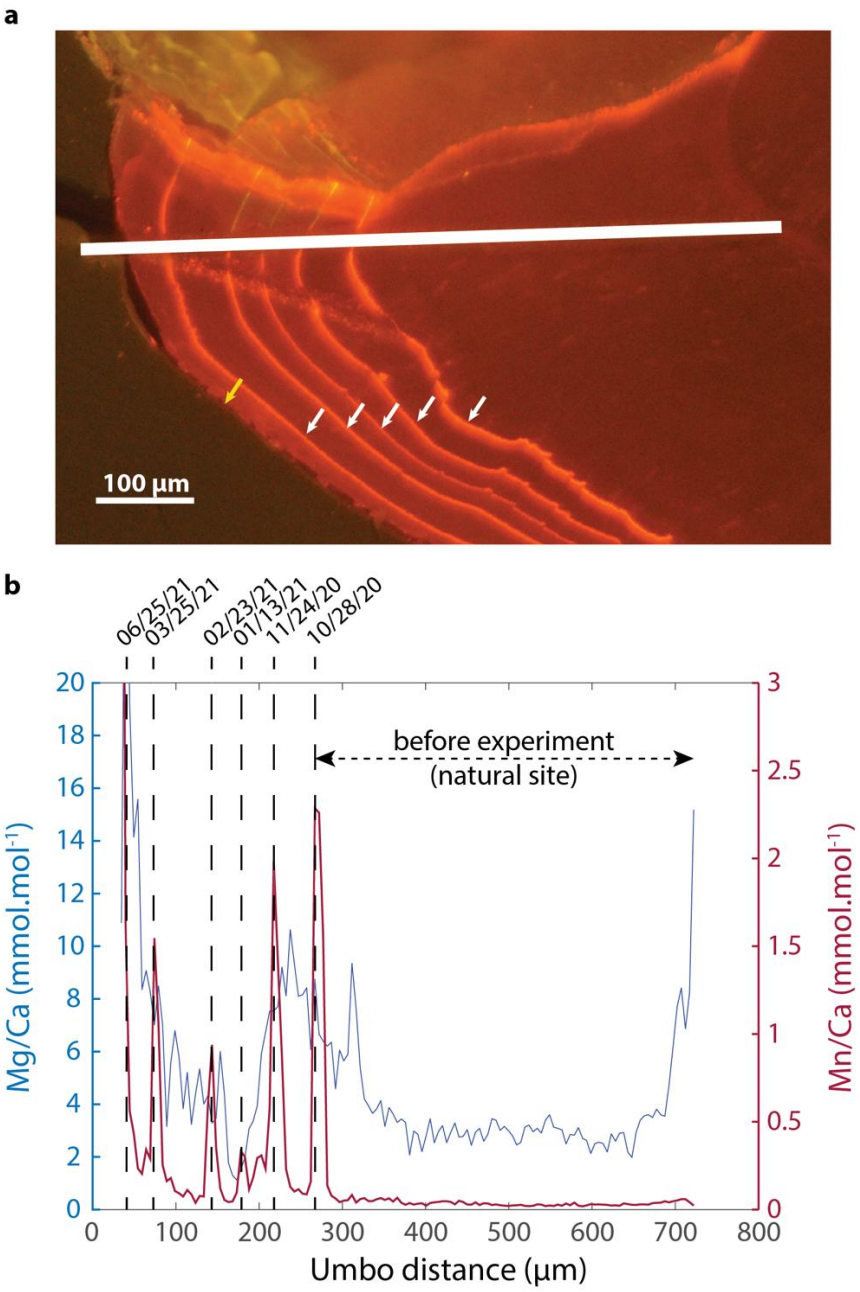

277
278

279 **Figure 4**: **Mn-labels on specimen G-308**. **a:** Cathodoluminescence view from thin
280 section on the last part of shell growth. Mn-labels are located by white arrows, and end
281 of life is located by the yellow arrow. A last Mn-label is not visible here due to low growth
282 rate between this label and end of life. The position of the LA-ICP-MS transect
283 corresponds to the white line. **b:** LA-ICP-MS transect of Mg/Ca and Mn/Ca following
284 direction indicated on **a**. The dates of all Mn-labels are indicated, based on the Mn/Ca
285 curve.

3.2. Geochemical analyses

3.2.1. Total elemental concentration in seawater and food

To assess the elemental composition of the oyster rearing environment, natural and artificial seawater samples were regularly collected from each aquarium and analyzed by inductively coupled plasma optical emission spectrometry (ICP-OES). These measurements focused on determining the concentrations of major elements, including Na, Mg, Al, K, Ca, Mn, Fe, Zn, Sr, and Ba in seawater. On average, 25 mL of water was sampled from each aquarium once per month, just before water renewal and oyster feeding. Additionally, a one-week daily monitoring (morning and afternoon) of the Mg concentration in ASW at the Paris rearing site was conducted to evaluate the impact of aquarium artificial seawater renewal on Mg concentration (**SI Table S11**).

Immediately after collection, seawater samples were acidified with 30 µL of nitric acid (HNO_3, 68% Normapur) and stored at +2°C in the dark until analysis. To distinguish between free and complexed form of Mg, each sample was divided into two portions: one half was filtered using a 2 µm Whatman 540 filter and diluted 1:200 in a 2% HNO_3 solution prepared with deionized water (resistivity: 18 MΩ·cm) for ICP-OES analysis, while the other half was kept to quantify free Mg by ion exchange chromatography (IEC).

To further evaluate Mg input from the oyster diet (*Instant Algae / Skeletonema*), we also characterized the elemental composition of the daily used solutions to feed *M. gigas* using ICP-OES. Approximately 5 mL of each nutritional solution was subjected to mineralization in 5 mL of 68% HNO_3 under continuous agitation for 12 hours to release intracellular elements. The solution was then filtered through a 2 µm Whatman 541 filter to confirm the absence of residual cellular material. If incomplete mineralization was observed, the nutritional solution was first diluted with deionized water before repeating the mineralization process. The fully processed samples were subsequently diluted in a 2% HNO_3 solution with a final dilution factor of 1:256 and stored with seawater samples at +2°C in the dark until analysis.

Elemental measurements were performed using an Agilent ICP-OES 5100 SVDV at the ALLIP6 analytical platform (Sorbonne University). Calibration was established using four

standard solutions of known elemental concentrations, which were analyzed before and after all sample runs to correct for potential instrumental drift and convert intensity signal to concentration. The standard solutions were also analyzed at a frequency of one per every 20 samples to monitor potential contamination. Additionally, blank samples were prepared and analyzed alongside experimental samples to verify the absence of contamination from reagents used in sample preparation (**SI Table S12**). Analytical uncertainties for each measured element were determined based on the standard deviation of three consecutive signal acquisitions from the same sample, along with internal standard repeatability. A full ICP-OES analysis report is available in **SI Table S12**.

3.2.2. Free Mg concentration in seawater

The proportion of free Mg (i.e., Mg^{2+} cation) in both natural (R1, R2 and R4) and artificial (P1, P2, P3) seawater was quantified using ion exchange chromatography (IEC). Due to the incompatibility of ethylenediaminetetraacetic acid (EDTA) with ion chromatography (Sharpe and London, 1997; Chumanov and Burgess, 2011), Mg^{2+} concentrations could not be determined for water samples from R3.

Acidified seawater samples were prepared for IEC analysis by dilution in deionized water at a 1:3000 ratio. To ensure data reliability, at least three replicates of each diluted sample were analyzed.

IEC measurements were performed at the Institute of Chemistry of Clermont-Ferrand (ICCF) using a Dionex ICS-6000 HPIC™ system equipped with a 2 × 250 mm IC column (Dionex IonPac™ CS-16). The Mg^{2+} concentration in eluted seawater samples was quantified via mass spectrometry using an ISQ™ EC Single Quadrupole Mass Spectrometer. Data integration and analysis were conducted with Chromeleon 7.2 software. Measurement reproducibility was accessed by analysing three replicates for each water sample (**SI Table S13**).

Finally, Mg^{2+} concentrations (i.e., $[Mg_{free}]$) obtained from IEC measurements were combined with total Mg concentrations (i.e., $[Mg_{tot}]$) from ICP-OES to calculate the fraction of complexed Mg (i.e., $[Mg_{complexed}]$) in seawater.

3.2.3. Shell elemental concentration by LA-ICP-MS

Chemical compositions of oyster shells were measured by laser-ablation inductively-coupled plasma mass spectrometry (LA-ICP-MS) at the Centre de Recherche en Archéologie, Archéosciences, Histoire (CReAAH, Université de Rennes, UMR 6566), with additional specimens analysed at the Institut des Sciences Analytiques et de Physico-Chimie pour l'Environnement et les Matériaux (IPREM, Université de Pau et des Pays de l'Adour). At CReAAH, the equipment used was an Agilent Technologies 7700 Series ICP-MS and a Cetac Technologies LSX-213 G2 (213 nm) laser ablation system. A total of 29 oyster specimens were analysed, including specimens that experienced different conditions along growth (**Table 1, SI 4**), separated by *in vivo* Mn-labelling. Analytical transects were performed such as crossing all Mn labels (observed with cathodoluminescence) using laser parameters as 25 µm spot size, 10 Hz frequency, 23 µJ at 10 µm.s^{-1}. At IPREM, we used an Agilent 8900 ICPMS Triple Quad coupled with a femtosecond laser ablation system (Novalase SA). This laser ablation system is equipped with a 2D galvanometric scanner which allows the 15 µm laser beam to move at high speed (1 mm.s^{-1}). Laser parameters for 20 µm-large transects were 200 Hz and 23 µJ at 5 µm.s^{-1}. Measured elements were ^{24}Mg, ^{55}Mn and ^{43}Ca as internal standard. Reference materials NIST SRM 610, 612 and 614 were analysed at the beginning, middle and end of each analytical session for calibration. Accuracy was checked using repeated measurements of otolith certified reference materials FEBS-1 and NIES-22. We used the preferred values of the GeoReM database (Jochum et al., 2005), when available. Data reduction for CReAAH analyses was performed on Matlab (http://www.mathworks.com) following the procedure described by Longerich et al. (1996). For IPREM analyses, data reduction was performed according to the same procedure using an inhouse program (FOCAL v. 2.46).

Table 1: **Number of specimens analysed by LA-ICP-MS and total analytical measurements for each experimental condition.** ASW: artificial seawater; NSW: natural seawater.

Experimental conditions		Number of measured specimens	Total number of measurements
P1	ASW, control	6	472
P2	ASW, +127 ppm $MgCl_2$	5	325
P3	ASW, +254 ppm $MgCl_2$	6	60
R1	NSW, control	5	415
R2	NSW, +127 ppm $MgCl_2$	6	268
R3	NSW, +127 ppm Mg-EDTA	5	165
R4	NSW, diet change	9	51

3.2.4. Data processing

Data processing was performed using Matlab (v. R.2023b; http://www.mathworks.com). The experimental condition intervals on the Mg/Ca transects were identified by localizing the *in vivo* labels from the Mn/Ca transects. The analytical measurement corresponding to the first label from each condition was not kept in the final data to avoid potential influence from previous conditions. The final number of analytical points is 1756. Normal distributions of shell Mg/Ca for each experimental condition were checked using Kolmogorov-Smirnov tests. For each test, a normal distribution was rejected at a 5% significance level (*p-value* < 0.0001). All distribution comparisons were therefore performed using Kruskal-Wallis non-parametric tests. We noted no significant differences between analytical platforms (Rennes and Pau) for each shell Mg/Ca condition groups (*p-values* > 0.05; **SI 5**) except for condition R1 with a weak significant difference (*p-value* = 0.0119). This small difference is probably caused by individual variability between specimens analysed. In order to avoid risking to lose this natural variability, we decided to keep all measurements as from the same distribution. Subsequent comparisons (as indicated in the rest of the manuscript) were performed without discrimination of the analytical platform. Multiple comparison procedure by Tukey method was used to identify homogeneity between experimental conditions for shell Mg/Ca.

4. Results

4.1. Monitoring of seawater physicochemical parameters

The average temperature and salinity for each rearing conditions are reported in **Table 2.** Over the seven-month experimental period, we observed fluctuation of seawater temperature between 18°C and 22°C at the Paris site, and between 17°C and 24°C at the Roscoff site (**SI 2**). These temperature fluctuations dont follow a clear seasonal pattern and are likely attributable to variations in the performance of the room's air conditioning systems. Although temperature changes occurred synchronously across the three tanks at each site, statistical analyses revealed consistent differences in average temperature between individual tanks (**SI 2**). On the Paris rearing site, tank P3 always shows an average temperature 0.7°C higher than that of tanks P1 and P2, while on the Roscoff site, tank R3 maintained an average temperature 0.7°C lower than that of tanks R1and R2/R4 (**Table 2**). Our experimental setup mimics open marine settings in terms of the absence of continental inputs. In such environmental settings and based on existing thermodependent Mg/Ca models in the literature (Mouchi et al., 2013), a shift of 0.7°C is expected to introduce a change of 0.31 $mmol.mol^{-1}$ in shell Mg/Ca. This change remains, however, negligible compared to the observed differences in shell Mg/Ca between conditions (**Table 2**).

Salinity monitoring at the Paris site, showed fluctuations of 32 to 40 psu, with an average value of 35.1 psu. The most pronounced changes were associated to the complete renewal of tank water (**SI Table S1**). Tank P2 shows significantly higher salinity than P1, which is consistent with the Mg enrichment it received (**Table 2**). On the opposite, P3 did not show a higher salinity than P2, despite it theoretically received a greater Mg enrichment.

Table 2: Summary of measurements performed on seawaters and shells for all experimental conditions.

	Seawater					Shells		
Condition	Temperature (°C)	Salinity (psu)	pH	Mg/Ca ($mmol.mol^{-1}$)	$[Mg]_{complexed}/[Mg]_{tot}$ (%)	Umbo growth rate (µm/day)	Average Mg/Ca ($mmol.mol^{-1}$)	Log D_{Mg}

P1	19.0±0.8	35±2	8.31±0.14	2.57±0.03	17.8 ± 6.0	1.09±0.40	7.02±4.32	0.436
P2	19.0±0.8	36±1	8.33±0.13	2.80±0.03	13.4 ± 6.3	1.16±0.69	7.87±3.71	0.449
P3	19.7±0.8	35±1	8.40±0.05	3.06±0.02	2.4 ± 1.8	0.64±0.38	9.44±5.39	0.489
R1	20.7±1.3	-	-	3.16±0.05	12.1 ± 5.6	1.41±0.98	5.72±2.54	0.258
R2	20.6±1.5	-	-	3.42	28.9 ± 4.8	1.43±0.83	8.40±5.56	0.390
R3	19.9±1.0	-	-	3.27±0.02	-	0.73±0.51	12.76±9.77	0.591
R4	20.5±1.0	-	-	3.17	0 ± 0.8	1.77±0.96	9.54±6.12	0.478

4.2. Growth rates and mortality

Over the seven-month experiment, mortality remained low across all rearing conditions except for R3, which received EDTA treatment. In conditions P1, P2, P3, R1, R2/R4, the first mortalities were recorded after six months and gradually increased toward the end of the rearing period (**SI S3, Figure S4**). In contrast, R3 exhibited a sharp increase in mortality, with 35.7% of oysters lost by day 35 of rearing and within the following 10 days, all *M. gigas* specimens in R3 died.

Based on CL observation, we found that the growth rate of the *M. gigas* umbos over the entire experimental period varied between 0.14 and 3.03 µm.day^{-1} across individuals (**SI 3, Table S8**). A comparative overview of average growth rates on the umbo of *M. gigas* grown under different conditions is presented in **Figure 5**. Kruskal-Wallis tests indicate no statistically significant differences in *M. gigas* growth between experimental groups (**SI 3**).

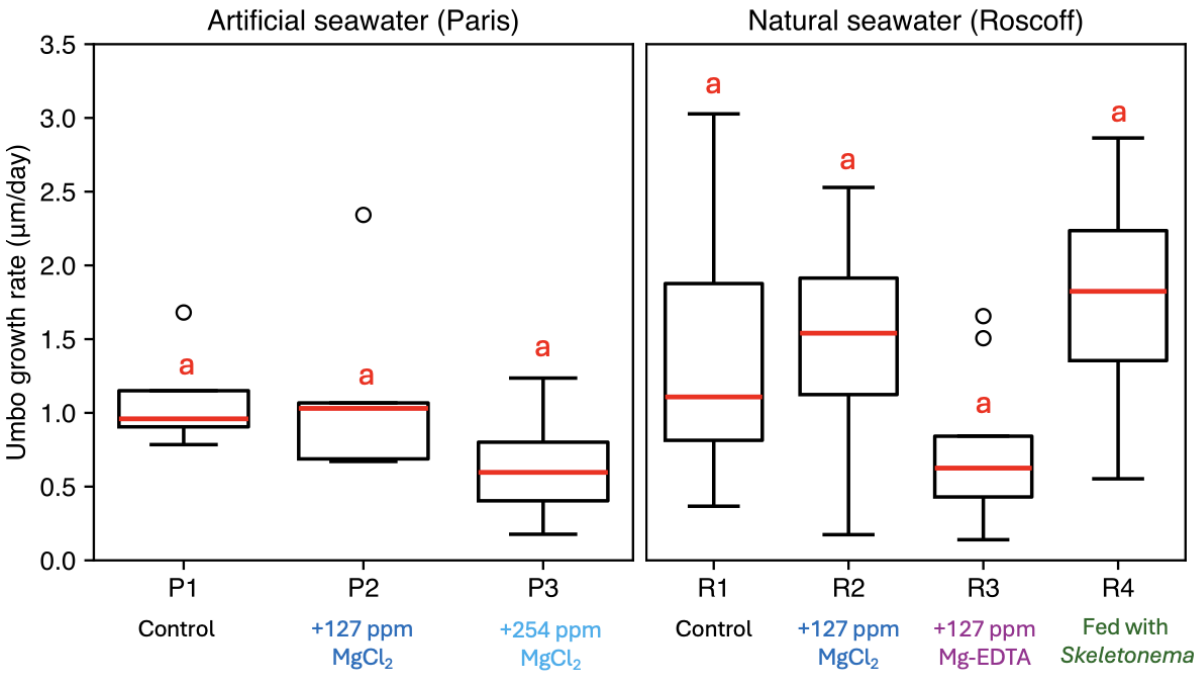

435

436 **Figure 5: Average growth rate of *M. gigas* umbo as a function of rearing conditions.**
437 Different letters on top of the boxes indicate significant differences between groups
438 based on Kruskal-Wallis test.

439

440 Periodic Mn labelling of oysters grown in P1 and P2 further allowed for the assessment of
441 growth rate evolution over the experimental period (**SI 3,** Figure S5). Although growth
442 rates between individuals exhibit some variability, the overall trend reveal a gradual
443 decline in *M. gigas* growth rate throughout the experiment (**SI 3,** Figure S5). This decline
444 coincided with increasing mortality across aquariums thought the end of the experiment,
445 which could be attributed to inadequate feeding of the oysters.

446

447 **4.3. Elemental concentration in seawater and food**

448 Across all the experimental conditions, total Mg and Ca concentrations in aquarium
449 seawater ranged from 1116 ppm to 1504 ppm and from 410 ppm to 592 ppm,
450 respectively. The average Mg and Ca concentrations for each condition are summarized
451 in **Table 3**.

452 **Table 3: Total Ca, Mg concentration measured by ICP-OES and free Mg concentration**
453 **measured by IEC in oyster's rearing seawater.** Concentrations are shown for each

condition as the average of all samples analyzed over the rearing period. The associated standard errors are given at 1σ.

Conditions		ICP-OES			IEC	
		N	$[Ca]_{tot}$ (ppm)	$[Mg]_{tot}$ (ppm)	N	$[Mg]_{free}$ (ppm)
P1	ASW	14	483 ± 9	1240 ± 16	2	1019 ± 62
P2	ASW	14	498 ± 9	1393 ± 32	2	1205 ± 62
P3	ASW	8	463 ± 9	1416 ± 20	1	1382 ± 7
R1	NSW	2	424 ± 7	1342 ± 5	2	1180 ± 71
R2	NSW	1	426	1504	1	1070 ± 73
R3	NSW	3	424 ± 6	1387 ± 11	0	Not analized
R4	NSW	1	410	1302	1	1316 ± 10

These results indicate that NSW contains more Mg and less Ca than ASW, resulting in a higher Mg/Ca ratio in NSW compared to ASW.

At the Paris rearing site, ICP-OES analyses revealed a gradual increase in Mg concentration in ASW from condition P1 to P3. While this trend confirms the successful artificial enrichment of Mg across different rearing conditions, the observed difference in Mg concentration between P1 and P3 (i.e., 176 ± 36 ppm) was notably lower than the expected 240 ppm. This also agrees with the salinity record, which shows no significant difference between P1 and P3 (**SI 2, Table S6**). Discrepancies were also observed for NSW conditions, where the difference in Mg content between R1 and R2 was higher than expected (i.e., 162 ppm compared to expected 127 ppm), while lower than anticipated between R1 and R3 (i.e., 46 ppm).

Daily monitoring of elemental concentrations in artificial seawater from the Paris aquariums showed that, on a weekly scale, variations in Mg and Ca concentrations remained relatively low (less than 110 ppm) and that periodic water renewal effectively maintained the target concentrations in each aquarium (**SI 6**). Additionally, salinity

measurements taken at the Paris site demonstrated no significant correlation between the Mg/Ca ratio of the seawater and salinity (**SI 6, Figure S7**).

Combined results of ICP-OES and IEC analyses further revealed that, even in EDTA-free conditions, complexed Mg accounts for 0% ± 0.8% to 29% ± 5% of total magnesium in both natural and artificial seawater (**Figure 6**). It is worth noting that the proportion of complexed Mg varied significantly across different conditions (**Figure 6**). For instance, conditions P1, P2, R1, and R2 contained substantial amounts of complexed Mg (ranging from 12% to 29%), whereas P3 and R4 showed little to no complexed Mg (**Table 2**).

Finally, ICP-OES analysis revealed significant differences in the Mg content of the two oyster feed solutions. *Instant Algae* contained approximately 112 ppm of Mg, whereas the *Skeletonema* solution had a markedly higher concentration of 4806 ppm Mg.

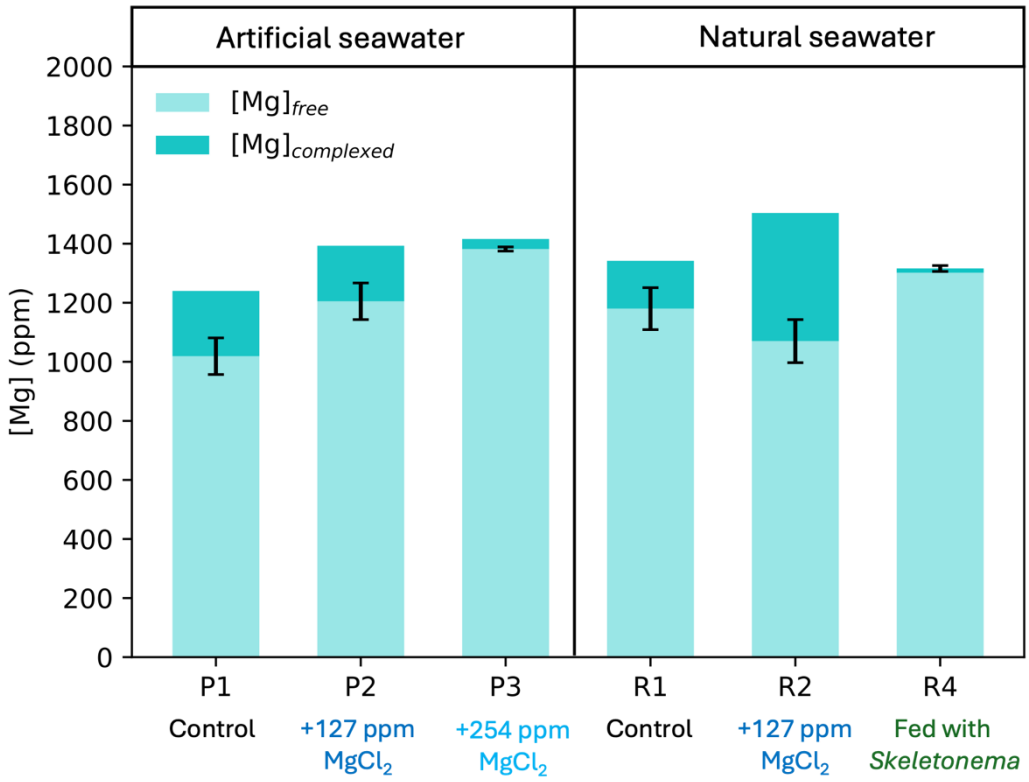

Figure 6: Histogram of the proportions of complexed (dark blue) versus free (light blue) magnesium in seawater as function of oyster rearing conditions.

4.4. Mg/Ca in oyster shells

The range for all shell Mg/Ca (**Figure 7**) extends from 0.31 to 51.80 mmol.mol^{-1}, with a median value of 6.26 mmol.mol^{-1} (mean = 7.56 mmol.mol^{-1}). For P1 group, shell Mg/Ca ranges from 1.10 to 28.58 mmol.mol^{-1}, with a median of 5.75 mmol.mol^{-1}. Shell Mg/Ca for P2 ranges from 0.70 to 22.74 mmol.mol^{-1}, with a median value of 7.19 mmol.mol^{-1}. P3 group values of shell Mg/Ca range from 3.33 to 26.94 mmol.mol^{-1}, with a median value of 7.78 mmol.mol^{-1}. For R1 group, values range from 1.47 to 14.98 mmol.mol^{-1} with a median value of 5.45 mmol.mol^{-1}. Shell Mg/Ca for R2 condition range from 0.31 to 31.56 mmol.mol^{-1} (median = 6.64). Shell Mg/Ca values for R3 condition range from 1.44 to 51.80 mmol.mol^{-1}, with a median value of 9.32 mmol.mol^{-1}. Mg/Ca values from R4 condition (diet change; no Mg enrichment) range from 0.71 to 46.55 mmol.mol^{-1} (median = 8.26). Shell Mg/Ca from P1 experimental condition is always significantly different than that of the other conditions (**Table 4**; **Figure 7**) including R1 condition, although both are control conditions in the experimental laboratories. Shell Mg/Ca from R1 is also significantly different than all other conditions. We note a significant influence of diet on shell Mg/Ca between commercial *Instant Algae* (R1) and fresh *Skeletonema* (R4; Kruskal-Wallis, *p-value* < 0.0001).

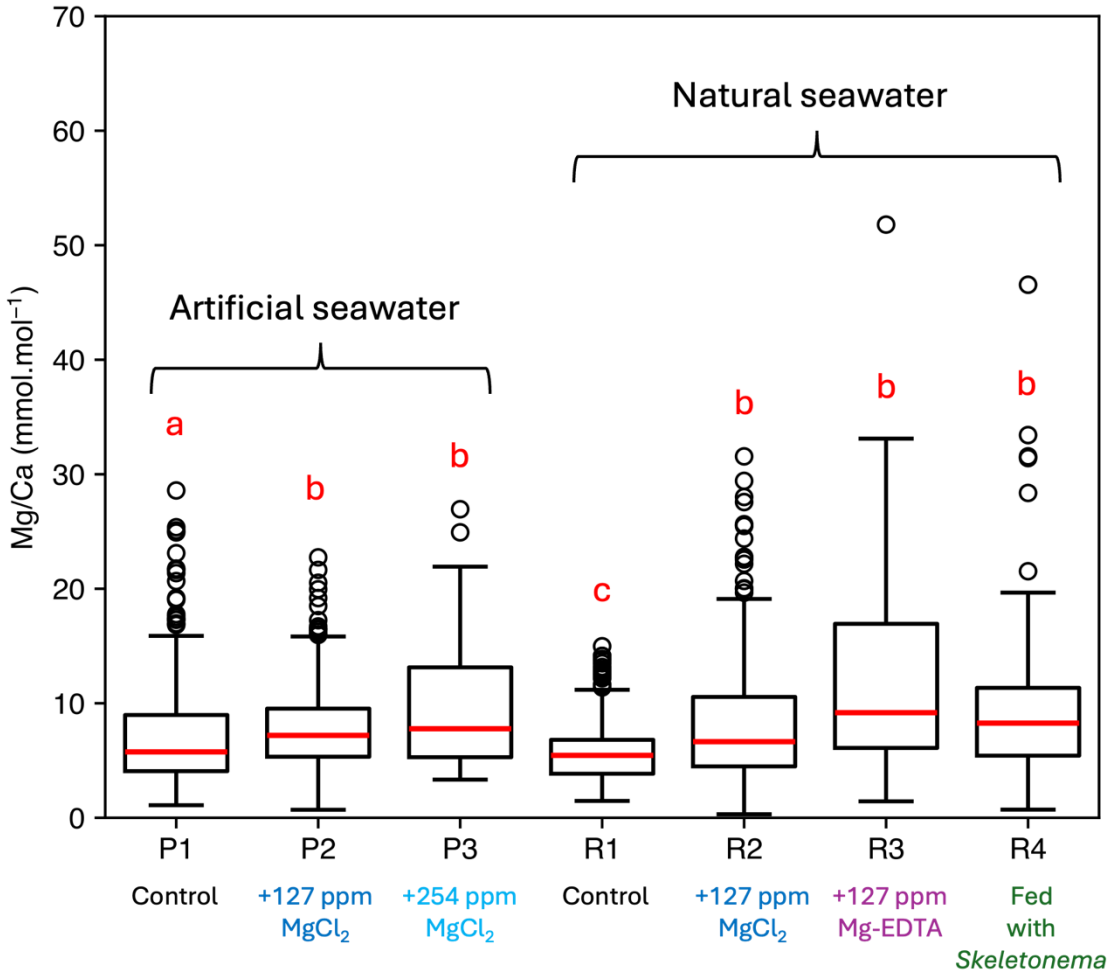

Figure 7: Boxplot of shell Mg/Ca for all experimental conditions. Different letters on top of the boxes indicate significant differences between groups (Tukey test).

Table 4: Result *p-values* from Kruskal-Wallis tests on shell Mg/Ca between the experimental conditions. Significant differences are highlighted in bold.

	P1	P2	P3	R1	R2	R3
P2	**< 0.0001**	-	-	-	-	-
P3	**0.0024**	0.8642	-	-	-	-
R1	**0.0023**	**< 0.0001**	**< 0.0001**	-	-	-
R2	**0.0087**	0.9609	0.5397	**< 0.0001**	-	-
R3	**< 0.0001**	0.0615	0.8360	**< 0.0001**	0.0139	-
R4	**< 0.0001**	0.2329	1.0000	**< 0.0001**	0.0370	0.8443

5. Discussion

5.1. Complexed Mg in seawater

Magnesium can exist in seawater in both free and complexed forms (Dyrssen and Edbord, 1974); however, direct quantification of these complexes has not yet been performed. In this study, we tested a simple but effective methodology, combining ICP-OES and ion exchange chromatography, to directly quantify complexed Mg in natural and artificial seawater in the oyster growth media.

Our results clearly confirm that, even in the absence of EDTA, a non-negligible fraction of Mg exists in its complexed form. On average, complexed Mg accounts for approximately 12.5% of total dissolved magnesium, a value consistent with previous theoretical estimates of inorganic Mg complexes in seawater (8% to 11%; Dyrssen and Edbord, 1974; Motekaitis and Martell, 1987).

Furthermore, the fact that complexed-Mg was found in similar proportions in both natural and artificial seawater suggests that these complexes are primarily inorganic in nature, and likely dominated by species like $MgOH^+$, $MgSO_4$, and $MgCO_3$ (Parkhurst and Appelo, 2013, Dyrssen and Edbord, 1974). However, we cannot entirely exclude a contribution from organic Mg complexes, potentially arising from the degradation of oyster-derived organic matter or food additives, which could vary between experimental conditions. This possibility is supported by observed variations in the proportion of complexed Mg between tanks (**Figure 6**), which could reflect differences in the concentration or stability of organic ligands under different rearing environments. Further information on the nature of the chemical species involved in complexation would be needed to confirm this hypothesis and to attribute the observed variations in Mg-complex concentration between tanks to specific rearing factors. To address this limitation, it would be valuable to combine our approach with complementary techniques such as FTIR or XANES, which could provide insights into the coordination environment of Mg and help distinguish between organic and inorganic complexes.

Overall, these findings demonstrate that the combination of ICP-OES and ion-exchange chromatography offers an effective tool to directly quantify complexed Mg in seawater. A

548 next step would be to apply this method to natural settings such as open-marine and
549 estuarine environments in order to verify the spatial and temporal variability of Mg
550 speciation.

551 **5.2. Influence of diet on shell Mg/Ca**

552 Although food is recognized as the primary source of essential elements for the
553 physiological functioning of marine organisms (Wang & Fisher, 1999; Reinfelder et al.,
554 1998), the effect of diet on elemental ratios recorded in shell had remain poorly studied.
555 The LA ICP-MS results from this study, revealed a significant shift in the Mg/Ca ratio of *M.*
556 *gigas* following change in diet (**Figure 7, Table 4**). Notably, *M. gigas* specimens exhibit a
557 systematic increase in Mg/Ca ratio after switching feeding solution from Instant Algae to
558 *Skeletonema* (**Figure 7, Table 2**). This finding strongly suggests that diet plays an
559 important role in modulating Mg incorporation in oyster shell.

560 Most studies on bivalve diets have focused on the effects of diet on growth. These studies
561 consistently show that both food quantity and quality can significantly influence shell
562 growth rates (e.g., Walne., 1976; Elsaesser, 2014). Since shell growth rate has also been
563 identified as a potential important factor influencing elemental incorporation into bivalve
564 shells (e.g., Schöne et al., 2011, Poulain et al., 2015; Lorrain et al., 2005; Freitas et al.,
565 2008, Vander Putten et al., 2000; Takesue & van Geen, 2004; Gillikin et al. 2005), it could
566 be hypothesized that dietary effects on shell Mg/Ca ratios may result from variations in
567 growth rates induced by changes in food quantity and/or quality. Nevertheless, this
568 hypothesis can be ruled out in our case, as we didn't observe any significant change in
569 growth rates between oysters grown in R1 and R4 (p-*value* > 0.05). Therefore, the
570 observed changes in shell Mg/Ca ratios between R1 and R4 must be attributable to a
571 direct influence of the dietary source on magnesium incorporation into the shell.

572 Furthermore, we observe that the difference in the shell Mg/Ca between R1 and R4
573 follows the Mg content of the respective feeding solutions, *Skeletonema* being enriched
574 in Mg compared to *Instant Algae*. This observation aligns with previous findings showing
575 that diatoms tend to have higher Mg concentrations compared to other phytoplankton
576 groups (Ho et al., 2003). In addition, differences in shell Mg/Ca between R1 and R4 (≈ 3.82
577 mmol.mol^{-1}) closely match those of the feeding solutions (≈ 3.24 mmol.mol^{-1}). While we

can't exclude that differences in digestion or assimilation efficiency of the two diets may also influence shell Mg/Ca, this founding strongly suggests that impact of diet on shell Mg/Ca is proportional to Mg content of the diet.

Overall, these results highlight that food is a major source of Mg for oyster shell, and diet also controls shell Mg/Ca. Failing to consider this effect may lead to inaccurate reconstructions of seawater temperature based on shell Mg/Ca, with errors on temperature estimated from 5.4°C to 14.4°C based on Mouchi et al. (2013) and Tynan et al. (2017) respectively. However, in open marine settings (model from Mouchi et al., 2013) food source should not vary as much compared to estuarine environments (model from Tynan et al., 2017) where both marine and continental nutrients are available (e.g., Xu et al., 2020). Consequently, bias on temperature reconstruction due to changes in food source should be substantially more pronounced in estuarine settings compared to open marine settings. Therefore, food source variability probably contributes to the divergence between environmental settings in Mg/Ca-T models (**Figure 8**).

5.3. Influence of Mg form and Mg/Ca of seawater on shell Mg/Ca

5.3.1. Complexed Mg in seawater remains bioavailable for oyster shell incorporation

The rearing experiment performed with natural seawater aimed at assessing the bioavailability of Mg when trapped in molecules with covalent bonds. Our results indicate that a higher concentration in seawater of identical proportions of free (R2 tank) and complexed Mg (R3 tank) induces a similar increased uptake of this element in oyster shells compared to control (R1 tank; **Table 3**). This implies that covalent bonds from chelators can be broken by the oysters to extract Mg, and possibly other elements, for metabolism functioning and shell incorporation.

This observation also explains the mortality observed in R3 tank. The commercial Mg-EDTA used here (TCI, ref. E0094) was chosen as it was stable when put in solution in deionized water, and exhibited a pH of 8 (*i.e.*, compatible with oyster rearing). By breaking the bonds between Mg and the EDTA molecule, oysters were releasing in their tissues ionic-form EDTA, which acted as a chelator to other elements, probably necessary for

609 their metabolism. Indeed, numerous chemical elements are cofactors to enzymes (*e.g.*,
610 Zn for carbonic anhydrase; Lee et al., 1995) or included in metal-binding proteins (*e.g.*,
611 Cu and Cd; Imber et al., 1987).
612
613 In natural settings, Mg uptake in shells is equivalent whether Mg is released from organic
614 ligands or directly available in free ionic form. Therefore, the Mg form in seawater does
615 not explain the variety of shell Mg/Ca values found in the literature (in oysters: Surge &
616 Lohmann, 2008; Mouchi et al., 2013; Tynan et al., 2017; in other bivalves: Wanamaker et
617 al., 2008; Schleinkofer et al., 2021; Mouchi et al., 2025b).

618 ***5.3.2. Higher concentration of Mg in seawater increases shell Mg/Ca***

619 Oysters reared in Mg-enriched (natural or artificial) seawater present higher shell Mg/Ca
620 than control specimens (**Fig. 7**, **Table 3**). A precise relationship between seawater Mg and
621 shell Mg/Ca is impossible to define with the present data, which present only two
622 increased concentrations of Mg (+127 ppm for tanks P2, R2 and R3; +254 ppm for tank
623 P3). It also remains unclear if the selected concentrations – of relatively low increase –
624 can have a substantial impact on shell Mg/Ca. Specimens from P3 appear to present
625 generally higher Mg/Ca than those from P2 (**Fig. 7**), yet no statistically significant
626 difference has been measured between these groups (**Fig. 7**; **Table 3**). Seawater samples
627 from P2 exhibit the expected Mg concentration (≈ 127 ppm increase compared to P1;
628 **Table 2**), but samples from P3 present lower Mg concentration compared to the expected
629 +254 ppm (≈ 200 ppm increase; **Table 2**). Still, the measured seawater Mg concentration
630 in P3 remains higher than that of P2, and that excess was however not sufficient to
631 significantly change the shell Mg/Ca.
632

633 ***5.3.3. Impact of seawater Mg/Ca on reconstructed temperatures***

634 A variety of bivalve shell Mg/Ca-temperature relationship has been suggested in the
635 literature, mainly from oysters and mussels (Mouchi et al., 2018). The range of values of
636 Mg/Ca can differ quite a lot between species and/or locality for the same temperature
637 settings: *e.g.*, 1-6 mmol.mol^{-1} (for *M. gigas* from France; Mouchi et al., 2013), 10-20

mmol.mol^{-1} (for *Mytilus edulis* from aquarium; Wanamaker et al., 2008), 10-40 mmol.mol^{-1} (*Acesta excavate* from deep-sea Norwegian Atlantic region; Schleinkofer et al., 2021). From various thermodependant Mg/Ca models from bivalves (**SI 7**), the closest reconstructed temperature to true temperatures (19.0°C for ASW; 20.7°C for NSW; **Table 4**) for the control from the ASW experiment (P1) corresponds to the model from Freitas et al. (2008) with 20.8°C, while the best fitted model for the control from the NSW experiment (R1) corresponds to that of Mouchi et al. (2013) with 23.4°C. This difference is likely due to contrasted seawater Mg/Ca between NSW and ASW. For the ASW experiment, a Mg^{2+} enrichment of 127 ppm (P2) and 254 ppm (P3) induces an increase in reconstructed temperatures of 3.2°C and 9.2°C, respectively. For the NSW experiment, a Mg^{2+} enrichment of 127 ppm (R2) induces an increase in reconstructed temperatures of 10.1°C, while the complexed Mg enrichment (R3) causes an increase of 26.6°C for reconstructed temperatures. The poor health condition of oysters from R3 is probably responsible of at least part of that important increase, as the EDTA released in their body has most probably negatively impacted a variety of metabolic biochemical processes. At this stage it is impossible to determine the extent of those impacts and the resulting changes in the chemistry of the extrapallial-fluid (EPF) from which shell precipitates. In particular, this can influence the pH and calcium saturation index of the EPF which have been reported to impact Mg/Ca in carbonates (e.g., Kisakürek et al., 2008; Mavromatis et al., 2017; Gray and Evans, 2019; Alvarez Caraveo et al., 2025, **Figure 8**), although other studies reported no significant impact of pH on shell Mg/Ca (e.g., Davis et al., 2017).

Based on both these experiments (NSW and ASW), we can assert that seawater Mg/Ca has a substantial impact on shell Mg/Ca (Figure 8), and therefore on reconstructed temperatures from models. This was previously suggested by Tynan et al. (2017), although the difference observed by the authors on seawater Mg/Ca between their two study areas was relatively low (between 5.3 and 5.6 – with one short drop at 4.6, and stable around 5.6 at Pambula Lake and Moreton Bay, respectively). As very few studies provide shell Mg/Ca – temperature models with values of seawater Mg/Ca (Surge & Lohmann, 2008; Tynan et al., 2017), a precise representation of the variety of seawater Mg/Ca in natural environments (in particular in open marine settings that our experiments mimic here, opposed to estuarine settings) is difficult to determine.

Here, seawater Mg/Ca ranges from 2.57 to 3.42 according to the experimental settings (**Table 2**), and is already responsible for quite important changes in shell Mg/Ca. Future works should be mindful to provide this information to evaluate with precision its impact.

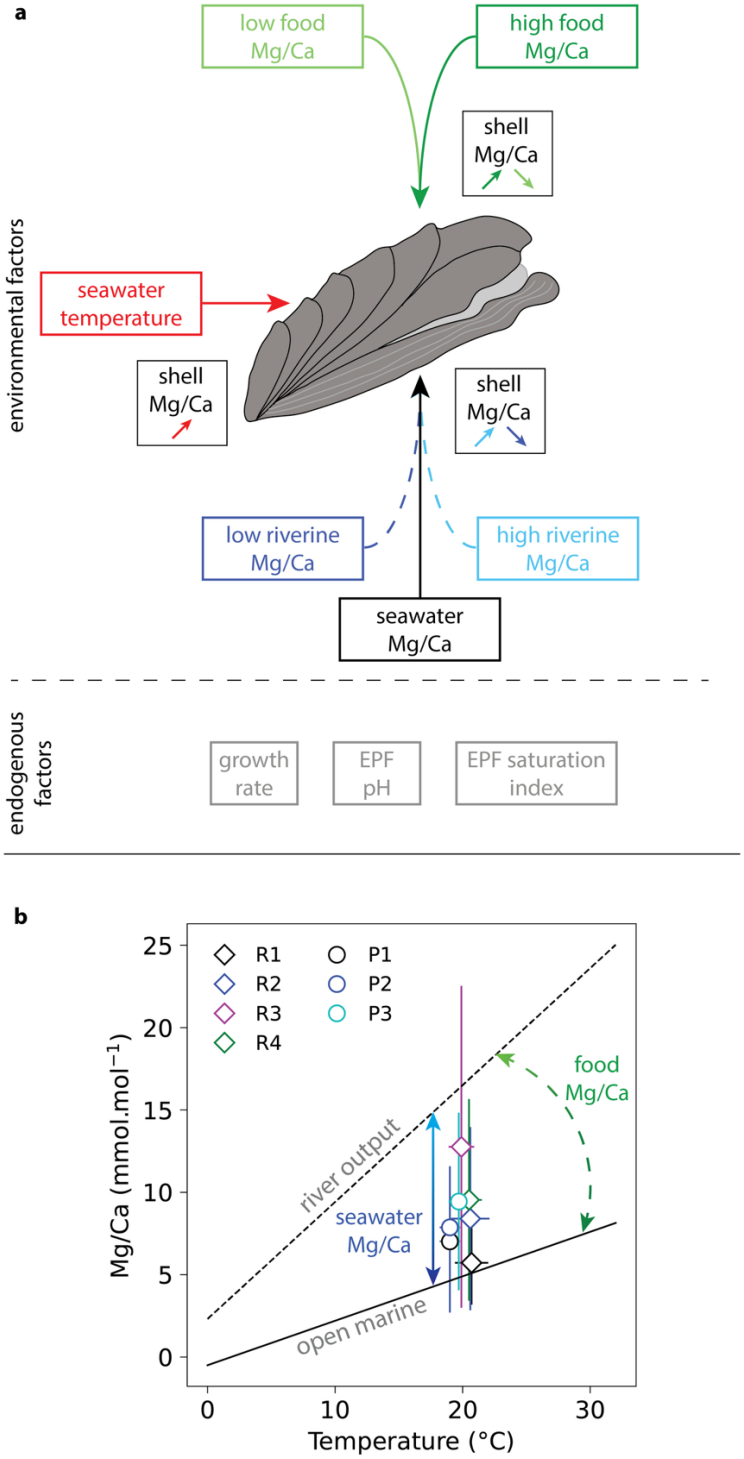

Figure 8: a) Suggested influences of environmental and endogenous factors on bivalve's shell Mg/Ca based on previous studies from the literature and data from this study. b) Suggested effect of seawater and food Mg/Ca on Mg/Ca – T models.

5.4. Potential factors explaining the discrepancies between Mg/Ca-T models and implications on temperature reconstructions

The Figure 8a summarises the environmental and endogenous factors influencing shell Mg/Ca. Although most previous studies in the literature have demonstrated the influence of temperature and some endogenous processes (vital effects) on Mg incorporation in bivalve shells (e.g., Gillikin et al., 2005; Lazareth et al., 2007; Schöne et al., 2011, 2013; Mouchi et al., 2013; Alvarez Caraveo et al., 2025), these processes are unlikely to explain the discrepancies of Mg/Ca-T models between marine and estuarine setting (**Figure 1**). Still, the results of this study clearly indicate the influence of additional environmental parameters on shells Mg/Ca. Notably, we found that both seawater Mg/Ca and food source can significantly affect shell Mg/Ca (**Figure 8b**). Those could be responsible for environmental specific Mg/Ca-T models.

As we demonstrated, shells Mg/Ca increase with seawater Mg/Ca. Therefore, on one hand, for similar environmental setting, we can assume that seawater Mg/Ca, primarily controls the models y-intercepts (Tynan et al., 2017, **Figure 8b**). On the other hand, the model slopes (specific to marine and estuarine environment) should be governed by other factors. In particular, we need to identify a seasonal environmental parameter whose expression is accentuated during summer in estuarine environments. Based on our results, a potential candidate would be a change of weighting in contributing food sources between marine and continental origins with distinct Mg/Ca ratios, since food Mg/Ca influence shell Mg/Ca. A similar interpretation was given for the distribution of $\delta^{13}C$ values of bivalve shells between marine and estuarine settings (Milano et al., 2019; Mouchi et al., 2020).

Overall, the estuarine environment harbours more variability in water and food sources influencing shell Mg/Ca than marine settings. Reconstruction of temperature using Mg/Ca of bivalve shells from open marine environments should be less biased.

Alternatively, shell Mg/Ca from estuarine settings carry additional information that can be deconvoluted to improve our knowledge on past coastal environments.

6. Conclusion

In this study we set up a culture experiment to investigated the influence of Mg form and source on shell Mg/Ca ratio. Our result, confirm the presence of complexed Mg in natural settings. Complexed Mg remains bioavailable and shell Mg/Ca varies with seawater Mg/Ca regardless of the Mg form (i.e., complexes or free ion). Food source also appears as a factor influence shell Mg/Ca with potential positive correlation between food Mg/Ca and shell Mg/Ca. As a result, we propose that further aquarium and in situ calibration studies should consider the seawater Mg/Ca and food Mg/Ca. Moreover, paleoenvironmental reconstructions based on Mg/Ca should choose appropriate models regarding the environmental settings of studied fossils.

Acknowledgements

This study was funded by the INSU TelluS INVISITE project. M.P. was funded by the Master grant from the Institut de l'Océan, Alliance Sorbonne Université. V.M. was funded by the ANR CERBERUS project (ANR-17-CE02-0003).

References:

Alvarez Caraveo, B., Guillermic, M., Downey-Wall, A., Cameron, L.P., Sutton, J.N., Higgins, J.A., Ries, J.B., Lotterhos, K., Eagle, R.A., 2025. Magnesium (Mg/Ca, δ^{26}Mg), boron (B/Ca, δ^{11}B), and calcium (Ca^{2+}) geochemistry of *Arctica islandica* and *Crassostrea virginica* extrapallial fluid and shell under ocean acidification. Biogeoscience 22, 12, 2831-2851.

Bougeois, L., de Rafélis, M., Reichart, G.-J., de Nooijer, L.J., Dupont-Nivet, G., 2016. Mg/Ca in fossil oyster shells as palaeotemperature proxy, an example from the Palaeogene of Central Asia. Palaeogeogr. Palaeoclimatol. Palaeoecol. 441, 611–626.

Briard, J., Pucéat, E., Vennin, E., Daëron, M., Chavagnac, V., Jaillet, R., Merle, D., de Rafélis, M., 2020. Seawater paleotemperature and paleosalinity evolution in

neritic environments of the Mediterranean Margin: insights from isotope analysis of bivalve shells. Palaeogeogr. Palaeoclimatol. Palaeoecol. 543, 109582.

Chauvaud, L., Lorrain, A., Dunbar, R.B., Paulet, Y-M., Thouzeau, G., Jean, F., Guarini, J-M., Mucciarone, D., 2005. Shell of the Great Scallop *Pecten maximus* as a high-frequency archive of paleoenvironmental changes. Geochem. Geophy. Geosyst. 6.

Chipman, W. A. 1966. Uptake and accumulation of chromium-51 by the clam, Tapes decussatus, in relation to physical and chemical form. In Disposal of Radioactive Wastes into Seas, Oceans and Surface Waters, Proc. Symp., Vienna, 16-20 May 1966, 571- 82. IAEA, Vienna, 898.

Chumanov, R.S. and Burgess, R.R., 2011. Artifact-inducing enrichment of ethylenediaminetetraacetic acid and ethyleneglycoltetraacetic acid on anion exchange resins. Anal biochem 412, 1, 34-39.

Davis, C.V., Fehrenbacher, J.S., Hill, T.M., Russell, A.D., Spero, H.J., 2017. Relationships between temperature, pH, and crusting on Mg/Ca ratios in laboratory-grown *Neogloboquadrina* foraminifera. Paleoceanogr. 32, 1137–1152.

Dyrssen, D., and Wedborg, M. 1974. Equilibrium calculations of the speciation of elements in sea water. The sea 5, 181-195.

Elsaesser, W.N. 2014. Influence of diet on element incorporation in the shells of two bivalve molluscs: *Argopecten irradians concentricus* and *Mercenaria mercenaria*. PhD dissertation, University of South Florida.

Epstein, S., Buchsbaum, R., Lowenstam, H.A. and Urey, H.C., 1953. Revised carbonate-water isotopic temperature scale. Geological Society of America Bulletin, 64, 1315-1326.

Freitas, P., Clarke, L., Kennedy, H., Richardson, C., 2008. Inter-and intra-specimen variability masks reliable temperature control on shell Mg/Ca ratios in laboratory and field cultured *Mytilus edulis* and *Pecten maximus* (Bivalvia). Biogeoscience Discussions 5, 1245-1258.

Gillikin, D.P., Lorrain, A., Navez, J., Taylor, J.W., André, L., Keppens, E., Baeyens, W., Dehairs F., 2005. Strong biological controls on Sr/Ca ratios in aragonitic marine bivalve shells. Geochem. Geophys. Geosyst. 6, Q05009.

769 Gray, W. R., Evans, D., 2019. Nonthermal influences on Mg/Ca in planktonic foraminifera:
770 a review of culture studies and application to the Last Glacial Maximum.
771 Paleoceanogr. Paleoclimatol. 34, 306–315.
772 Hausmann, N., Siozos, P., Lemonis, A., Colonese, A.C., Robson, H.K., Anglos, D., 2017.
773 Elemental mapping of Mg/Ca intensity ratios in marine mollusc shells using Laser-
774 Induced Breakdown Spectroscopy. J. Anal. At. Spectrom. 32, 8, 1467–1472.
775 Hirose, K. 2006. Chemical speciation of trace metals in seawater : a review. *Anal. Sci* 22,
776 1055-1063.
777 Ho, T.-Y., Quigg, A., Finkel, Z.V., Milligan, A.J., Wyman, K., Falkowski, P.G., Morel, F.M.M.,
778 2003. The elemental composition of some marine phytoplankton. J. Phycol. 39, 6,
779 1145-1159.
780 Hunter, K.A., Boyd, P.W., 2007. Iron-binding ligands and their role in the ocean
781 biogeochemistry of iron. Environ. Chem. 4, 4, 221-232.
782 Huyghe, D., Lartaud, F., Emmanuel, L., Merle, D., Renard, M., 2015. Palaeogene climate
783 evolution in the Paris Basin from oxygen stable isotope ($\delta^{18}O$) compositions of
784 marine molluscs. J. Geol. Soc. 172, 5, 576–587.
785 Huyghe, D., de Rafélis, M., Ropert, M., Mouchi, V., Emmanuel, L., Renard, M., Lartaud, F.,
786 2019. New insight into oyster high-resolution shell growth patterns. Marine Biology
787 166, 48.
788 Imber, B.E., Thompson, J.A.J., Ward, S., 1987. Metal-binding protein in the Pacific Oyster,
789 *Crassostrea gigas*: assessment of the protein as a biochemical environmental
790 indicator. Bull Environ Contam and Toxicol 38, 707-714.
791 Jochum, K.P., Nohl, U., Herwig, K., Lammel, E., Stoll, B., Hofmann, A.W., 2005. GeoReM:
792 a new Geochemical Database for Reference Materials and isotopic standards.
793 Geostand. Geoanal. Res. 29, 333–338.
794 Kirby, M. X., Soniat, T. M. and Spero, H. J. 1998. Stable isotope sclerochronology of
795 Pleistocene and recent oyster shells (*Crassostrea virginica*). Palaios 13, 560–569.
796 Klein, R.T., Lohmann, K.C., Thayer, C.W, 1996. Bivalve skeletons record sea-surface
797 temperature and $\delta^{18}O$ via Mg/Ca and $^{18}O/^{16}O$ ratios. Geology 24, 415–418.
798 Kısakürek, B., Eisenhauer, A., Böhm, F., Garbe-Schönberg, D., Erez, J., 2008. Controls on
799 shell Mg/Ca and Sr/Ca in cultured planktonic foraminiferan, *Globigerinoides ruber*
800 (white). Earth Planet. Sci. Lett. 273, 3–4, 260-269.

Langlet, D., Alunno-Bruscia, M., Rafélis, M.D., Renard, M., Roux, M., Schein, E. and Buestel, D., 2006. Experimental and natural cathodoluminescence in the shell of Crassostrea gigas from Thau lagoon (France): ecological and environmental implications. Mar. Ecol. Prog. Ser. 317, 143-156.

Lartaud, F., de Rafelis, M., Ropert, M., Emmanuel, L., Geairon, P. and Renard, M., 2010. Mn labelling of living oysters: artificial and natural cathodoluminescence analyses as a tool for age and growth rate determination of *C. gigas* (Thunberg, 1793) shells. Aquaculture 300, 1-4, 206-217.

Lartaud, F., Emmanuel, L., De Rafélis, M., Ropert, M., Labourdette, N., Richardson, C. A., Renard, M. 2010. A latitudinal gradient of seasonal temperature variation recorded in oyster shells from the coastal waters of France and The Netherlands. Facies 56, 13-25.

Lazareth, C.E., Guzman, N., Poitrasson, F., Candaudap, F., Ortlieb, 2007. Nyctemeral variations of magnesium intake in the calcitic layer of a Chilean mollusk shell (*Concholepas concholepas*, Gastropoda). GCA 71, 5369-5383.

Le Corre, P., Tréguer, P., Courtot, P. 1972. Evaluation de matière organique dissoute dans des eaux côtières de la Bretagne méridionale en avril 1970. Cahier de Biologie Marine 13, 443-455

Lee, J., Morel, F., 1995. Replacement of zinc by cadmium in marine phytoplankton. Mar. Ecol. Prog. Ser. 127, 305–309.

Longerich, H.P., Jackson, S.E., Günther, D., 1996. Inter-laboratory note. Laser ablation inductively coupled plasma mass spectrometric transient signal data acquisition and analyte concentration calculation. J. Anal. At. Spectrom. 11, 899-904.

Lorrain, A., Gillikin, D.P., Paulet, Y.M., Chauvaud, L., Le Mercier, A., Navez, J., Andreì, L. 2005. Strong kinetic effects on Sr/Ca ratios in the calcitic bivalve *Pecten maximus*. Geology 33, 12, 965–968.

Marchand, M. 1974. Considérations sur les formes physico-chimiques du cobalt, manganèse, zinc, chrome et fer dans l'eau de mer enrichie ou non en matière organique. *J. Cons. Int. Explor. Mer* 35, 2, 130-142.

Mavromatis, V., Immenhauser, A., Buhl, D., Purgstaller, B., Baldermann, A., Dietzel, M., 2017. Effect of organic ligands on Mg partitioning and Mg isotope fractionation

during low-temperature precipitation of calcite in the absence of growth rate effects. Geochim. Cosmochim. Acta 207, 139-153.

Milano, S., Schöne, B.R., Gutierrez-Zugasti, I., 2019. Oxygen and carbon stable isotopes of *Mytilus galloprovincialis* Lamarck, 1819 shells as environmental and provenance proxies. The Holocene, 30, 65-76.

Motekaitis, R.J., Martell, A.E., 1987. Speciation of metals in the oceans. I. Inorganic complexes in seawater, and influence of added chelating agents. Mar. Chem. 21, 2, 101-116.

Mouchi, V., de Rafélis, M., Lartaud, F., Fialin, M., Verrecchia E., 2013. Chemical labelling of oyster shells used for time-calibrated high resolution Mg/Ca ratios: a tool for past estimation of seasonal temperature variations. Palaeogeogr. Palaeoclimatol. Palaeoecol. 373, pp. 66-74.

Mouchi, V., Briard, J., Gaillot, S., Argant, T., Forest, V., Emmanuel, L., 2018. Reconstructing environments of collection site from archaeological bivalve shells: case study from oysters (Lyon, France). J. Archaeol. Sci. Rep., 21, 1225-1235.

Mouchi, V., Emmanuel, L., Forest, V., Rivalan, A., 2020. Geochemistry of bivalve shells as indicator of shore position of the 2nd c. BC. Open Quat. 6, 4, 1-15.

Mouchi, V., Andrus, C.F.T., Checa, A.G., Elliot, M., Griesshaber, E., Hausmann, N., Huyghe, D., Lartaud, F., Peharda, M., de Winter, N.J., 2025. Oyster shells as archives of present and past environmental variability and life history traits: A multi-disciplinary review of sclerochronology methods and applications. L&O Letters 10, 179-199.

Mouchi, V., Nedoncelle, K., Bruguier, O., Le Bris, N., Garmirian, Z., Lartaud, F., 2025. Mg/Ca from mussel shells rather than $\delta^{18}O$ as a promising temperature proxy for hydrothermal vent ecosystems. Deep-Sea Res. I: Oceanogr. Res. Pap. 219, 104485.

Parkhurst, D.L., Appelo, C.A.J., 2013. Description of input and examples for PHREEQC version 3—a computer program for speciation, batch-reaction, one-dimensional transport, and inverse geochemical calculations. USGS TM 6(A43), 497.

Pierre, C., 1999. The oxygen and carbon isotope distribution in the Mediterranean water masses. Mar. Geol. 153, 41-55.

Pouil, S., Metian, M., Dupuy, C., Teyssié, J.L., Warmau, M., Bustamante, P. 2020. Diet variably affects the trophic transfer of trace elements in the oyster *Crassostrea gigas*. Mar. Environ. Res. 161, 105124.

Poulain, C. Gillikin, D.P., Thébault, J., Munaron, J.M., Bohn, M., Robert, R., Paulet, Y.-M., Lorrain, A., 2015. Chem. Geol. 396, 42-50.

Purton L. and Brasier M. 1997. Gastropod carbonate $\delta^{18}O$ and $\delta^{13}C$ values record strong seasonal productivity and stratification shifts during the late Eocene in England. Geology 25, 10,871–874.

Reinfelder, J.R., Fisher, N.S., Luoma, S.N., Nichols, J.W., Wang, W.X. 1998. Trace element trophic transfer in aquatic organisms: a critique of the kinetic model approach. Sci. Total Environ 219, 117-135

Rohling, E.J., 2000. Paleosalinity: confidence limits and future applications. Mar. Geol. 163, 1–11.

Schleinkofer, N., Raddatz, J., Evans, D., Gerdes, A., Flögel, S., Voigt S., Büscher, J.V., Wisshak, M., 2021. Compositional variability of Mg/Ca, Sr/Ca, and Na/Ca in the deep-sea bivalve *Acesta excavata* (Fabricius, 1779). PLoS ONE, 16, e0245605.

Schöne, B.R., Gillikin, D.P., 2013. Unraveling environmental histories from skeletal diaries — advances in sclerochronology. Palaeogeogr. Palaeoclimatol. Palaeoecol. 373, 1–5.

Schöne, B. R., Zhang, Z., Radermacher, P., Thébault, J., Jacob, D. E., Nunn, E. V. & Maurer, A.-F., 2011. Sr/Ca and Mg/Ca ratios of ontogenetically old, long-lived bivalve shells (*Arctica islandica*) and their function as paleotemperature proxies. *Palaeogeogr, Palaeoclimat, Palaeoecol* 302, 52–64.

Schöne, B.R., Radermacher, P., Zhang, Z., Jacob, D.E. 2013. Crystal fabrics and element impurities (Sr/Ca, Mg/Ca and Ba/Ca) in shells of *Arctica islandica* – Implication for paleoclimate reconstructions. Palaeogeogr. Palaeoclimatol. Palaeoecol. 373, 50-59.

Shaked, Y., Lis, H., 2012. Disassembling iron availability to phytoplancton. Front. Microbiol. 3, 123.

Sharpe, J.C., London, E., 1997. Inadvertent concentrating of EDTA by ion exchange chromatography: avoiding artifacts that can interfere with protein purification. Anal. Biochem. 250, 124-125.

895 Surge, D., Lohmann, K.C., 2008. Evaluating Mg/Ca ratios as a temperature proxy in the
896 estuarine oyster, *Crassostrea virginica*. J. Geophys. Res. 113, G02001.
897 Takesue, R.K., Van Geen, A., 2004. Mg/Ca, Sr/Ca, and stable isotopes in modern and
898 holocene *Protothaca staminea* shells from a northern California coastal upwelling
899 region. Geochim. Cosmochim. Acta, 68, 3845–3861.
900 Tynan, S., Dutton, A., Eggins, S., Opdyke, B., 2014. Oxygen isotope records of the
901 Australian flat oyster (*Ostrea angasi*) as a potential temperature archive. Mar.
902 Geol. 357, 195-209.
903 Tynan, S., Opdyke, B.N., Walczak, M., Eggins, S., Dutton, A. 2017. Assessment of Mg/Ca
904 in *Saccostrea glomerata* (the Sydney rock oyster) shell as a potential temperature
905 record. Palaeogeogr. Palaeoclimatol. Palaeoecol. 484, 79-88.
906 Ullmann, C.V., Wiechert, U., Korte, C., 2010. Oxygen isotope fluctuations in a modern
907 North Sea oyster (*Crassostrea gigas*) compared with annual variations in seawater
908 temperature: Implications for palaeoclimate studies. Chem. Geol. 277, 160-166.
909 Urey, H.C., Lowenstam, H.A., Esptein, S., McKinney, C.R., 1951. Measurement of
910 paleotemperatures and temperatures of the Upper Cretaceous of England,
911 Denmark, and the Southeastern United States. GSA Bulletin 62, 4, 399-416.
912 Uvanovic, H., Schöne, B.R., Markulin, K., Janekovic, I., Peharda, M., 2021. Venerid bivalve
913 *Venus verrucosa* as a high-resolution archive of seawater temperature in the
914 Mediterranean Sea. Palaeogeogr. Palaeoclimatol. Palaeoecol. 561, 110057.
915 Vander Putten, E., Dehairs, F., Keppens, E., Baeyens, W., 2000. High resolution
916 distribution of trace elements in the calcite shell layer of modern *Mytilus edulis*:
917 environmental and biological controls. Geochim. Cosmochim. Acta, 64, 6, 997-
918 1011.
919 Wafar, M., Le Corre, P., 1982, Evolution saisonnière de la matière organique dissoute
920 dans les eaux côtières de la Manche Occidentale (Baie de Morlaix): Evolution
921 simultanée du Carbone, de l'Azote et du Phosphore organique dissous. CNEXO
922 Actes Colloq., 14, 47-66.
923 Walne, P.R., 1976. Experiments on the culture in the sea of the Butterfish Venerupis
924 decussata L. Aquaculture, 8, 371-381.
925 Wanamaker, A.D., Kreutz, K.J., Wilson, T., Borns Jr. H.W., Introne, D.S., Feindel, S. 2008.
926 Experimentally determined Mg/Ca and Sr/Ca ratios in juvenile bivalve calcite for

Mytilus edulis: implications for paleotemperature reconstructions. Geo-Mar. Lett. 28, 359-368.

Wang, W.X., Fisher, S.N. 1999. Assimilation efficiencies of chemical contaminants in aquatic invertebrates: A synthesis. Environ. Toxicol. Chem. 18. 9, 2034-2045.

Wefer, G., Berger, W.H., 1991. Isotope paleontology: growth and composition of extant calcareous species. Mar. Geol. 100, 207-248.

WMO, 2025. https://wmo.int/topics/climate, World Meteorological Organization website, consulted on 05/21/25.

Xu, L., Yang, D., Greenwood, J., Feng, X., Gao, G., Qi, J., Cui, X., Yin, B., 2020. Riverine and oceanic nutrients govern different algal bloom domain near the Changjiang Estuary in summer. Journal of Geophysical Research: Biogeosciences 125: e2020JG005727. https://doi.org/10.1029/2020JG005727.

Zhang, J., Kattner, G., Koch, B.P., 2019. Interaction of trace elements and organic ligands in seawater and implications for quantifying biogeochemical dynamics: A review. Earth-Sci. Rev. 192, 631-649.

Supplementary Information on “Impact of sources and forms of Mg on oyster shell Mg/Ca”

Marie Pesnin[1,2*], Laurent Emmanuel[1], Amélie Guittet[1], Boris Eyheraguidel[3], Gaëtan Schires[4], Vincent Mouchi[5,6,7]

[1]: Sorbonne Université, CNRS-INSU, Institut des Sciences de la Terre Paris, ISTeP, F-75005, Paris, France
[2]: Geowissenschaftliches Zentrum, Georg–August–Universität Göttingen, 37077, Göttingen, Germany.
[3]: ?
[4]: ?
[5]: Sorbonne Université, CNRS, Adaptation et Diversité en Milieu Marin, AD2M, Station Biologique de Roscoff, 29680, Roscoff, France
[6]: CNRS, CReAAH, Université de Rennes, Rennes Cedex, France
[7]: Sorbonne Université, CNRS, Laboratoire d’Ecogéochimie des Environnements Benthiques, LECOB, Observatoire Océanologique, F-66650, Banyuls-sur-mer, France

1. Labelled oyster shell from the rearing experiment

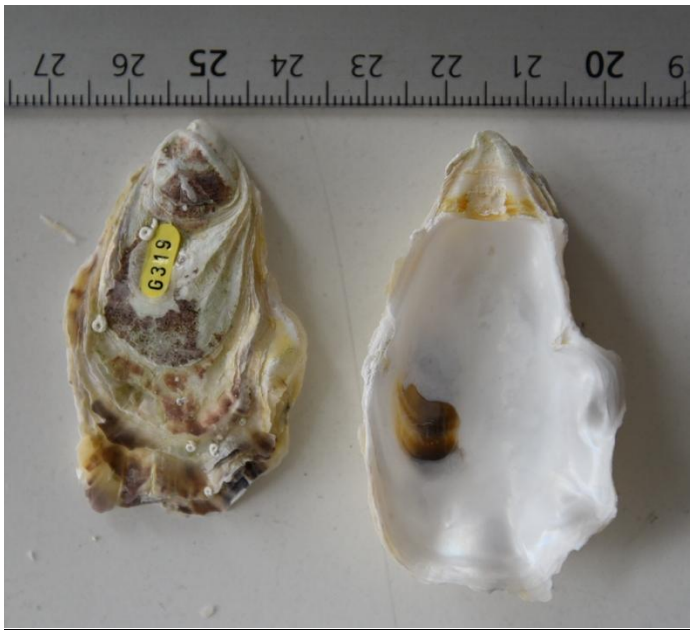

Figure S1 : Photo of the shell of one oyster specimen G.319 reared in artifical seawater sacrificed for geochemical measurements after removing the soft tissue from the organism and cleaning the shell from organic residute with oxygen peroxyde.

2. Monitoring of physicochemical parameters of seawater in rearing tanks

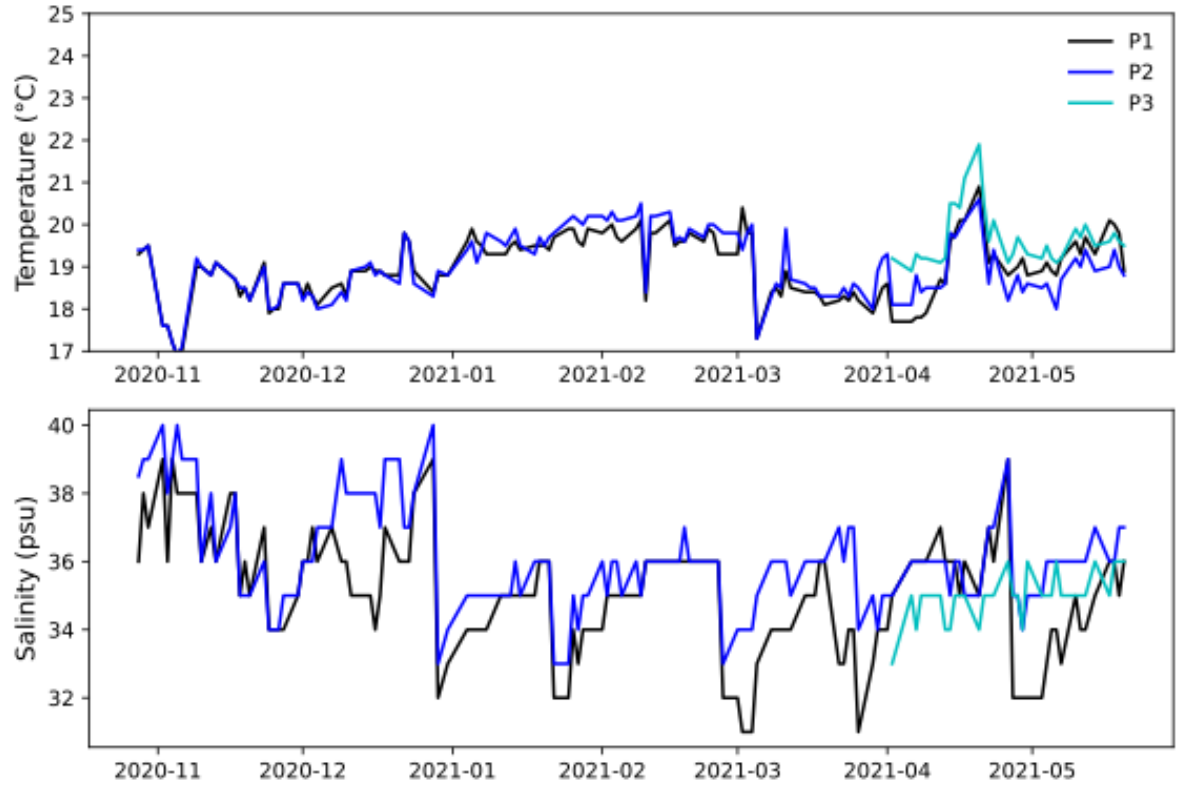

Figure S2: Daily recording of temperature (°C), salinity (‰) and pH of artificial seawater in aquariums as a function of culture conditions.

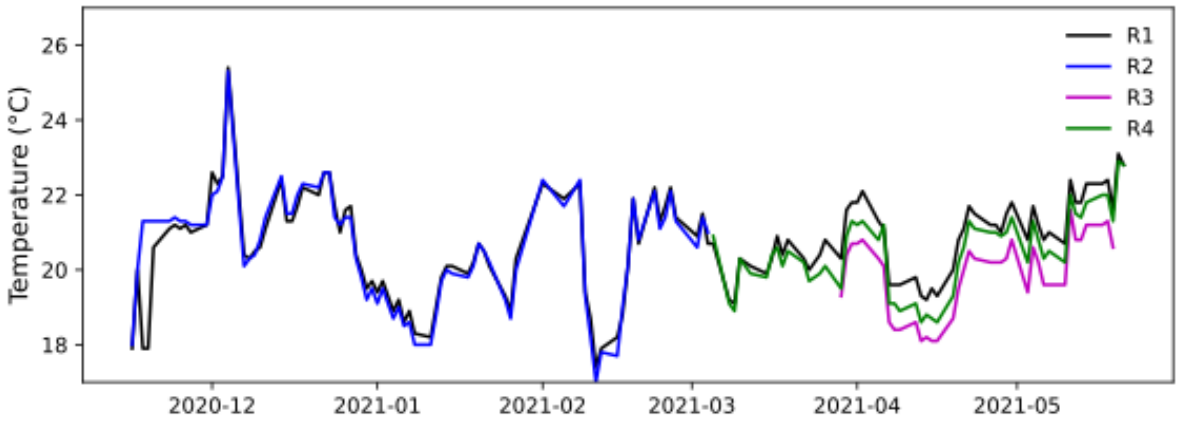

Figure S3: Daily recording of temperature (°C) natural seawater in aquariums as a function of culture conditions.

	P1	P2
P2	0.9506	-

P3	$1.784\ 10^{-4}$	$3.859\ 10^{-4}$

Table S3: Results for Kruskal-Wallis tests performed to test the null hypothesis that, for each experimental condition in the Paris (ASW) experiment and for the entire experimental period, the seawater temperature comes from the same distribution.

	P1	P2
P2	0.2054	-
P3	0.0165	$2.582\ 10^{-5}$

Table S4: Results for Kruskal-Wallis tests performed to test the null hypothesis that, for each experimental condition in the Paris (ASW) experiment and for the period during which all conditions were run simultaneously, the seawater temperature comes from the same distribution.

	R1	R2	R3
R2	0.9816	-	-
R3	0.0043	0.0234	-
R4	0.6744	0.8936	0.1562

Table S5: Results for Kruskal-Wallis tests performed to test the null hypothesis that, for each experimental condition in the Roscoff (NSW) experiment, the seawater temperature comes from the same distribution.

	P1	P2
P2	$4.847\ 10^{-6}$	-
P3	0.6193	$2.892\ 10^{-4}$

Table S6: Results for Kruskal-Wallis tests performed to test the null hypothesis that, for each experimental condition in the Paris (ASW) experiment and for the entire experimental period, the seawater salinity comes from the same distribution.

	P1	P2
P2	0.0107	-
P3	0.5613	$2.634\ 10^{-4}$

Table S7: Results for Kruskal-Wallis tests performed to test the null hypothesis that, for each experimental condition in the Paris (ASW) experiment and for the period during

which all conditions were run simultaneously, the seawater salinity comes from the same distribution.

3. Growth rate and mortality of *M. gigas* over the culture experiment

Table S8: Growth rate of *M. gigas* oyster umbo under culture conditions, determined from cathodoluminescence observations.

ID	*Conditions*	*Starting date*	*End date*	*Total days*	*Umbo length (µm)*	*Growth rate (µm/day)*
G.302	P1	28/10/2020	24/05/2021	208	196,7	0,95
G.308	P1	28/10/2020	15/07/2021	260	204,0	0,78
G.314	P1	28/10/2020	11/06/2021	226	220,0	0,97
G.324	P1	28/10/2020	19/05/2021	203	341,2	1,68
G.333	P2	28/10/2020	23/07/2021	268	276,2	1,03
G.334	P2	28/10/2020	24/05/2021	208	139,5	0,67
G.352	P2	28/10/2020	15/07/2021	260	277,5	1,07
G.355	P2	28/10/2020	24/05/2021	208	143,1	0,69
G.360	P2	28/10/2020	24/05/2021	208	487,2	2,34
G.365	P3	02/04/2021	26/07/2021	115	20,4	0,18
G.373	P3	02/04/2021	29/07/2021	118	75,7	0,64
G.375	P3	02/04/2021	08/05/2021	36	12,8	0,35
G.383	P3	02/04/2021	08/05/2021	36	30,8	0,85
G.374	P3	02/04/2021	24/05/2021	52	28,7	0,55
G.388	P3	02/04/2021	24/05/2021	52	64,3	1,24
G.075	R1	16/10/2020	29/03/2021	164	125,6	0,77
G.054	R1	16/10/2020	29/03/2021	164	157,1	0,96
G.096	R1	16/10/2020	19/05/2021	215	270,6	1,26
G.129	R1	16/10/2020	29/03/2021	164	341,6	2,08
G.032	R1	16/10/2020	19/05/2021	215	650,9	3,03
G.124	R1	16/10/2020	17/05/2021	213	78,2	0,37
G.071	R2	16/10/2020	29/03/2021	164	266,8	1,63
G.116	R2	16/10/2020	29/03/2021	164	302,5	1,84
G.012	R2	16/10/2020	05/03/2021	140	24,4	0,17
G.053	R2	16/10/2020	05/03/2021	140	40,3	0,29

G.056	R2	16/10/2020	29/03/2021	164	230,1	1,40
G.087	R2	16/10/2020	05/03/2021	140	297,0	2,12
G.127	R2	16/10/2020	05/03/2021	140	203,6	1,45
G.016	R2	16/10/2020	05/03/2021	140	354,0	2,53
G.013	R3	29/03/2021	10/05/2021	42	63,3	1,51
G.055	R3	29/03/2021	10/05/2021	42	5,9	0,14
G.071	R3	29/03/2021	10/05/2021	42	35,4	0,84
G.075	R3	29/03/2021	09/05/2021	41	18,2	0,44
G.116	R3	29/03/2021	09/05/2021	41	34,3	0,84
G.054	R3	29/03/2021	19/05/2021	51	12,0	0,24
G.056	R3	29/03/2021	19/05/2021	51	21,7	0,43
G.127	R3	29/03/2021	17/05/2021	49	81,1	1,66
G.129	R3	29/03/2021	17/05/2021	49	39,0	0,80
G.016	R3	29/03/2021	10/05/2021	42	19,1	0,46
G.012	R4	05/03/2021	19/05/2021	75	41,5	0,55
G.053	R4	05/03/2021	19/05/2021	75	214,8	2,86
G.087	R4	05/03/2021	19/05/2021	75	121,6	1,62
G.016	R4	05/03/2021	29/03/2021	24	48,6	2,03

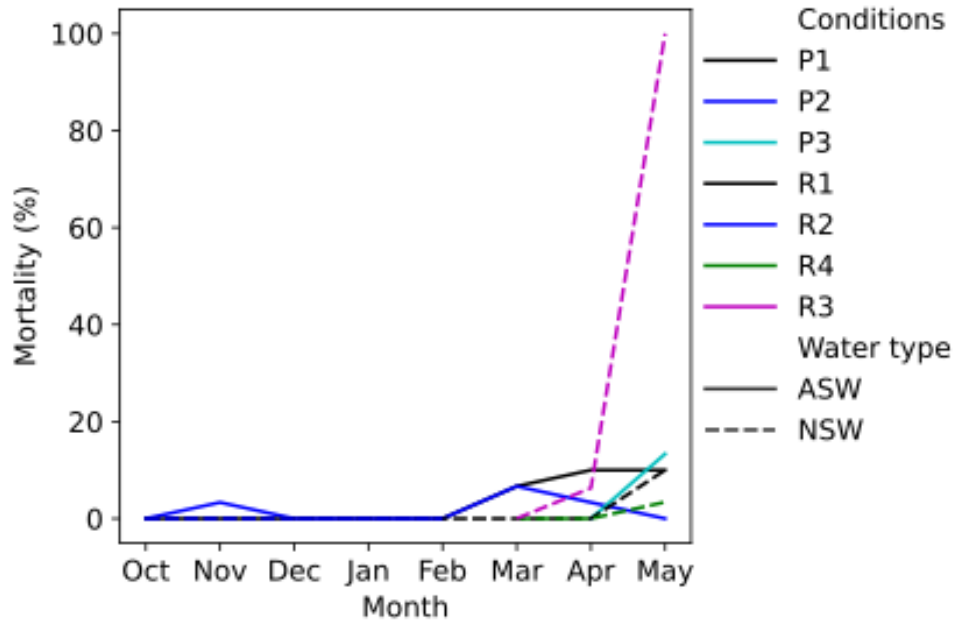

Figure S4: Monitoring of *M. gigas* mortality over rearing experiment.

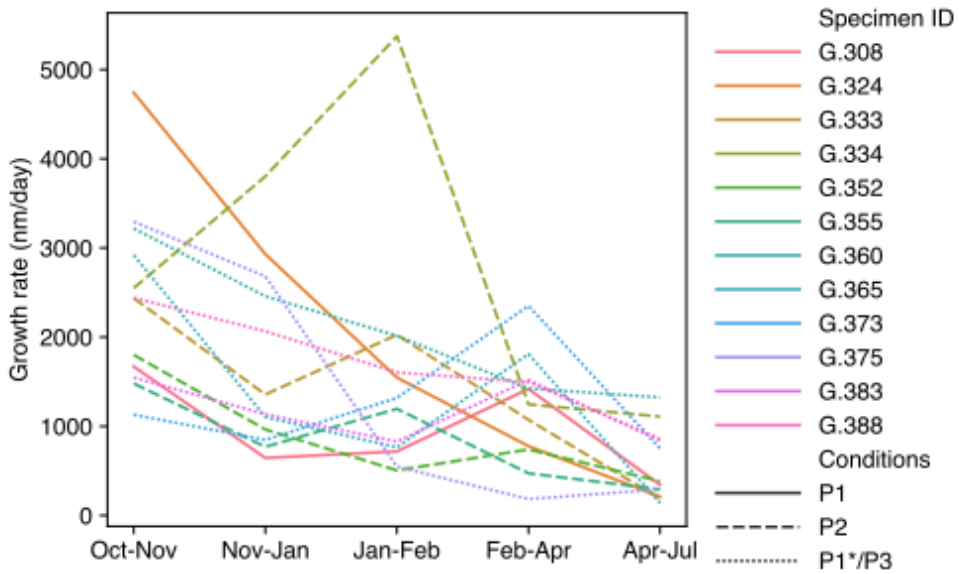

Figure S5: Evolution of the growth rate on the umbo of *M. gigas* specimens raised in artificial seawaters along the culture experiment.

Table S9: Results for Kruskal-Wallis tests performed to test the null hypothesis that, for each experimental condition in the Paris (ASW) experiment, the umbo growth rate comes from the same distribution.

	P1	P2
P2	0.9999	-
P3	0.5031	0.4061

Table S10: Results for Kruskal-Wallis tests performed to test the null hypothesis that, for each experimental condition in the Roscoff (NSW) experiment, the umbo growth rate comes from the same distribution.

	R1	R2	R3
R2	0.9995	-	-
R3	0.4915	0.3419	-
R4	0.9124	0.9335	0.2064

4. Experimental conditions for all analysed specimens

Table S14: Oyster specimens analysed by LA-ICP-MS and their respective experimental conditions during the experiment. Some specimens have been transferred during the experiment from one condition to another, after *in vivo* Mn-labelling.

ID	*Conditions*
G.012	R4
G.013	R3
G.016	R1, R3
G.053	R2, R4
G.054	R1, R3
G.055	R3
G.056	R2, R4, R3
G.071	R2, R3
G.075	R1
G.087	R2, R4
G.096	R1
G.116	R2, R3
G.127	R2, R3
G.129	R1, R3
G.302	P1
G.308	P1
G.314	P1
G.324	P1
G.333	P2
G.334	P2
G.352	P2
G.355	P2
G.360	P2
G.365	P3
G.373	P3
G.374	P3
G.375	P3
G.383	P3
G.388	P3

5. Comparison of shell Mg/Ca between analytical platforms

Table S15: Results for Kruskal-Wallis tests performed to test the null hypothesis that, for each experimental condition measured at both analytical platforms (CReAAH and IPREM), the shell Mg/Ca comes from the same distribution.

Conditions	***p-value***
P1	0.0851
P2	0.3299
P3	0.3804
R1	0.0119
R2	0.1105
R4	0.0722
R3	0.1218

6. Impact of seawater renewal on Mg concentration in seawater

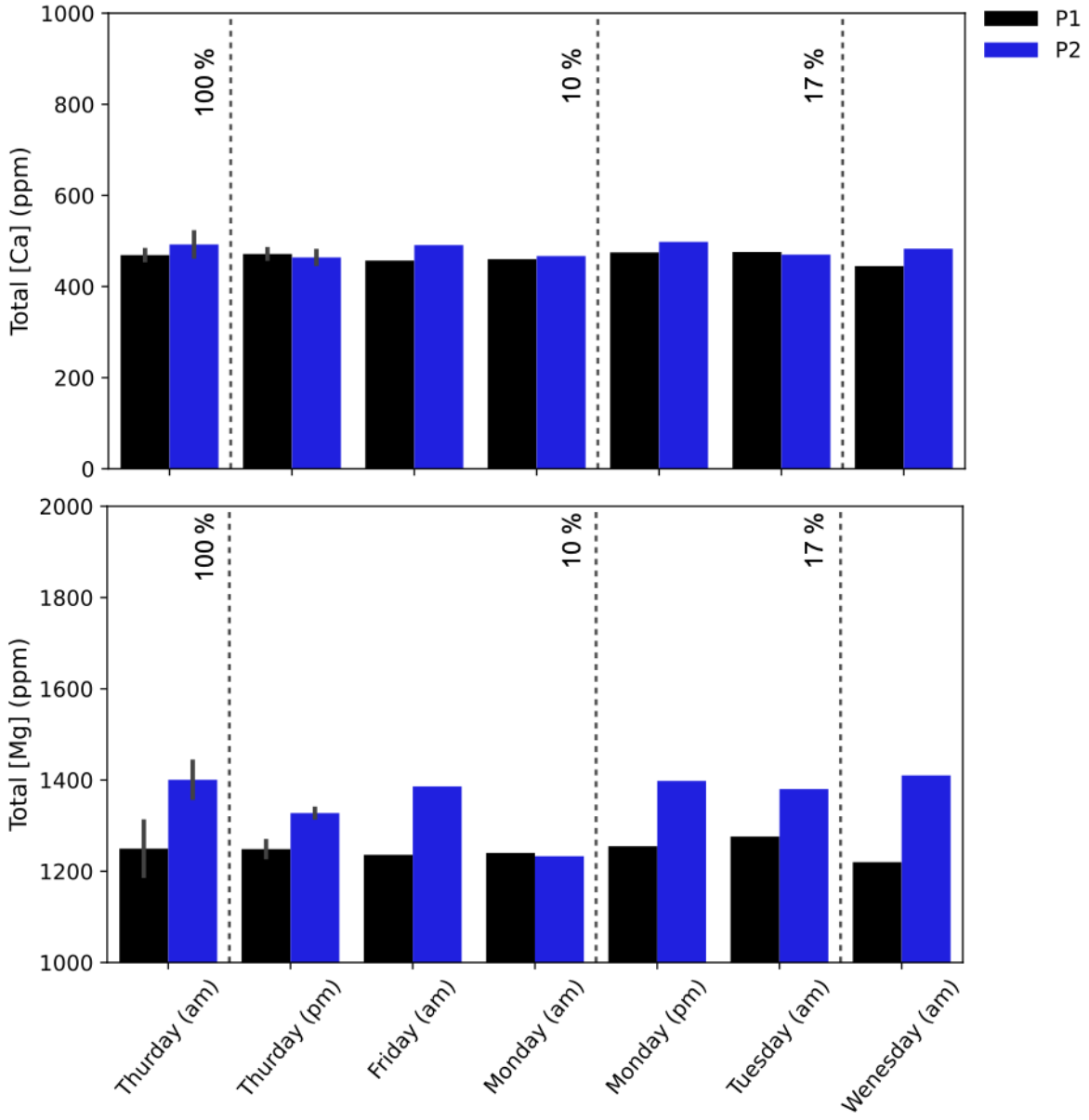

Figure S6: Daily evolution of calcium (top panel) and magnesium (bottom panel) concentrations in P1 (dark bars) and P2 (blue bars) aquaria before (am) and after (pm) seawater renewal. The percentage corresponds to the percentage of renewed water in the aquariums.

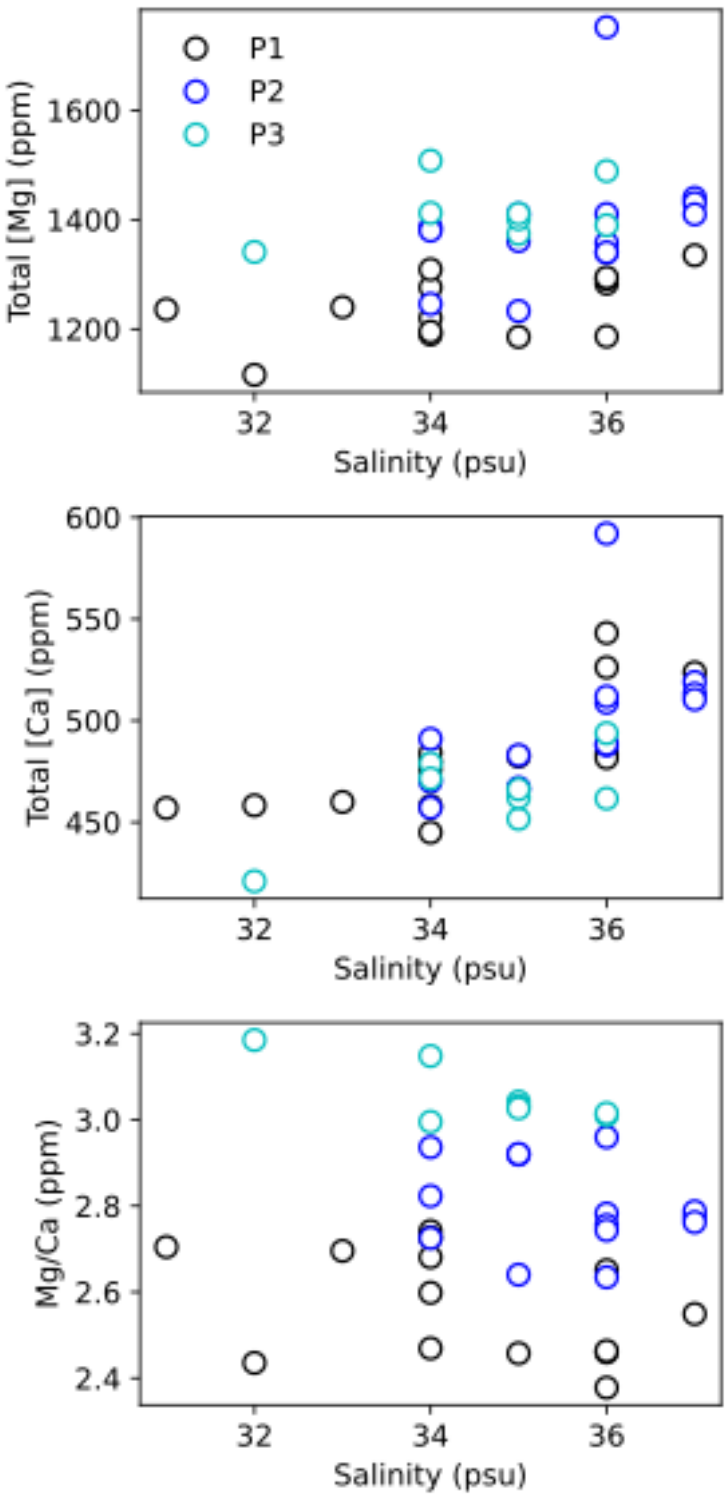

Figure S7: Evolution of [Ca], [Mg] and Mg/Ca ratio of the artificial seawater sampled from P1, P2 en P3 conditions as function of salinity.

7. Impact of seawater Mg enrichment on reconstructed temperatures

We present here the reconstructed temperatures by several thermodependant Mg/Ca models from oysters (Surge & Lohmann, 2008; Mouchi et al., 2013; Tynan et al., 2017) and mussels (Klein et al., 1996; Vander Putten et al., 2000; Freitas et al., 2008) from our natural (NSW: R1-R4) and artificial (ASW: P1-P3) seawater experiments. As seawater Mg/Ca is different between both experiments, comparisons should be made separately. For the study from Tynan et al. (2017), we used the equation from Moreton Bay as it corresponds to marine settings, which fit better to our experimental setup.

	P1	**P2**	**P3**	**R1**	**R2**	**R3**	**R4**
Shell Mg/Ca ($mmol.mol^{-1}$) [difference from control]	7.02 [-]	7.87 [0.85]	9.44 [2.42]	5.72 [-]	8.40 [2.68]	12.76 [7.04]	9.54 [3.82]
Reconstructed temperature – Klein et al. (1996): T = (Mg/Ca - 2.25) / 0.3 [difference from control]	15.9°C [-]	18.7°C [2.8°C]	24.0°C [8.1°C]	11.6°C [-]	20.5°C [8.9°C]	35.0°C [23.4°C]	24.3°C [12.7°C]
Reconstructed temperature – Vander Putten et al. (2000): T = (Mg/Ca + 0.63) / 0.7 [difference from control]	10.9°C [-]	12.1°C [1.2°C]	14.4°C [3.5°C]	9.1°C [-]	12.9°C [3.8°C]	19.1°C [10.0°C]	14.5°C [5.4°C]
Reconstructed temperature – Freitas et al. (2008): T = (Mg/Ca – 1.503) / 0.265 [difference from control]	20.8°C [-]	24.0°C [3.2°C]	30.0°C [9.2°C]	15.9°C [-]	26.0°C [10.1°C]	42.5°C [26.6°C]	30.3°C [14.4°C]
Reconstructed temperature – Surge & Lohmann (2008): T = (Mg/Ca + 0.23) / 0.72 [difference from control]	10.1°C [-]	11.3°C [1.2°C]	13.4°C [3.3°C]	8.3°C [-]	12.0°C [3.7°C]	18.0°C [9.7°C]	13.6°C [5.3°C]
Reconstructed temperature – Mouchi et al. (2013): T = (Mg/Ca * 3.77) + 1.88 [difference from control]	28.3°C [-]	31.5°C [3.2°C]	37.5°C [9.2°C]	23.4°C [-]	33.5°C [10.1°C]	50.0°C [26.6°C]	37.8°C [14.4°C]
Reconstructed temperature – Tynan et al. (2017) Moreton Bay: T = (Mg/Ca - 2.31) / 0.71 [difference from control]	6.6°C [-]	7.8°C [1.2°C]	10.0°C [3.4°C]	4.8°C [-]	8.6°C [3.8°C]	14.7°C [9.9°C]	10.2°C [5.4°C]

Table S16: Reconstructed temperatures from shell Mg/Ca of this study based on models from the literature. Differences (in °C) from control (P1 and R1 conditions) are indicated under brackets.